Modeling nonlinear response from distributed damage and kissing bonds

Koen van Den Abeele, Steven Delrue, Sylvain Haupert, Vladislav Aleshin

Modeling nonlinear response from distributed damage and kissing bonds

Koen Van Den Abeele*, Steven Delrue, Sylvain Haupert and Vladislav Aleshin

***Corresponding author's address: Physics, Wave Propagation and Signal Processing, KU Leuven, KULAK, Kortrijk, 8500, West-Flandres, Belgium, Koen.VanDenAbeele@kuleuven-kulak.be**

A large number of models have been proposed in the field of nonlinear elastic wave propagation in damaged solids to validate experimental observations with theoretical predictions. In this contribution, we distinguish between "distributed" and "interface" implementations of nonlinearity, and deduce particular properties for the differing models. For the models of distributed damage, we prove that many of the currently suggested models can be seen as particular cases of the PM-model for specific protocols and parameters. In addition, we illustrate the potentiality of interface models to validate experimental results reported by other research groups.

I. Introduction:

The investigation of nonlinear and non-unique stress-strain relations at the zone of damage constitutes the basics of ultrasonic Non-Destructive Testing (NDT) and modeling of nonlinear wave propagation in damaged solids. A large number of differing models have been proposed and used in the past to validate experimental observations with theoretical predictions, and vice-versa, in the field of nonlinear elastic wave propagation in damaged solids [1-23]. The state relations are usually defined at the microscopic or mesoscopic level, and their influence on the wave propagation is investigated on the macroscopic level by way of analytical models or finite difference and finite element models.

Models for nonlinear state relations generally include contributions known as classical stress-strain nonlinearity or atomic anharmonicity (mainly for mono-crystalline solids) [1], and a hysteretic contribution of the strain with respect to the stress variations attributed to the presence of soft inclusions in a stiff matrix [2,4,5,3,6,12,13,14,15,17]. The classical nonlinear contribution is commonly described by a perturbation expansion of stress in terms of strain (or vice-versa) in which only the first two or three terms are considered. To introduce hysteretic behavior, non-classical terms have to be added to the model, accounting for history and memory effects, such as the quite general Preisach-Mayergoysz (PM) model and derivatives of this model [13-20]. Most hysteretic models only account for fast/immediate stress-strain variations. Moreover, only the variations matter, not the rate at which the variations occur. Some exclusive extensions of these models make use of stochastic processes to account for experimentally observed features such as slow dynamics [24-27].

Depending on the nature of the damage, globally distributed or highly localized, the implementation of the nonlinear and hysteretic relations occurs at the level of a "representative volume" or at an "interface". In the first case, the damage zone can be considered as an ensemble of tiny nonlinear features (microcracks or dislocations), statistically spread over a certain volume. In the "interface model", single crack or delamination clapping behavior is insinuated [28-42].

In the next sections, we will discuss several state-of-the-art models that have been proposed in the past to validate experimental observations of nonlinear wave propagation in damaged solids. We will distinguish between "distributed" and "interface" implementation, and deduce particular properties for each of them. For the models of distributed damage, we prove that many of the currently suggested models can be seen as particular cases of the PM-model for specific protocols and parameters.

II. Models for distributed damage:

1. Preisach-Mayergoysz model

One of the most generic and most flexible models for the description of a nonlinear and hysteretic stress-strain relation at the mesoscopic level (representative volume level) is certainly the Preisach-Mayergoysz model (introduced by Ortin et al for shape memory alloys [13] and by Guyer et al. for rock mechanics [15], based on the original Preisach-Mayergoysz formalism for magnetism). In short, the formalism makes use of a statistical distribution of elementary hysteretic units that can be in two states, say state "0" and "1". The driving variable, say "*x*", determining the unit's state, can be either the stress or the strain. For each unit, the switch between the two states occurs at two parameter values of the driving variable, say x_0 for a change from state 0 to state 1 upon increasing *x*, and x_1, for a change from state 1 to state 0 when reducing *x*. These switching values are characteristic for each unit individually. A large amount of such units defines a density, expressed as function of the two switching parameters: $\rho_x\left(x_0, x_1\right)$. Based on physical arguments one can state that the density is only non-zero for $x_0 \geq x_1$. Apart from the hysteretic units, the representative volume also consists of elastic units which have a reversible (non-hysteretic) nonlinear state relation. Their behavior is characterized by the acousto-elastic effect (dynamic modulus, or wavespeed, versus drive parameter) and can be expressed as $K_{EU}\left(x\right)$. The knowledge of the density, together with the acousto-elastic effect is sufficient to determine the stress-strain equations for any kind of protocol "*h(x)*" of the drive parameter.

As such, we obtain the following expressions for the incremental variation of strain as function of stress, when the drive parameter is the stress:

$$\left[d\varepsilon\right]_{\sigma_A \to \sigma_B} = \int_{\sigma_A}^{\sigma_B} \frac{1}{K_{EU}(\sigma)} d\sigma \quad + \quad \gamma\left[f_\sigma\left(\sigma_B;h\right) - f_\sigma\left(\sigma_A;h\right)\right] \tag{1}$$

or for the incremental stress variation as function of strain, when the drive parameter is the strain.:

$$\left[d\sigma\right]_{\varepsilon_A \to \varepsilon_B} = \int_{\varepsilon_A}^{\varepsilon_B} K_{EU}(\varepsilon) d\varepsilon \quad + \quad K_0\gamma\left[f_\varepsilon\left(\varepsilon_B;h\right) - f_\varepsilon\left(\varepsilon_A;h\right)\right] \tag{2}$$

Here the function $f_x\left(x_j;h\right)$ represents the fraction of hysteretic units within the representative volume that are in state 1 at the value of the drive parameter corresponding to the function's argument, given the past history (*h*) of the protocol. Hysteresis comes into play by the fact that the fraction of units in state 1 depends on the history of the protocol of the drive parameter, and not only on its current value. The parameter γ, introduced above is the strain contribution from hysteresis when all hysteretic units are in state 1. Likewise, $K_0\gamma$ is the stress contribution occurring

when all hysteretic units are in state 1. Here K_0 denotes the linear modulus (first term in the series expansion of $K_{EU}(x)$).

In order to rewrite the hysteretic contributions in terms of the PM density, we introduce the notation N_∞ representing the total number of hysteretic units (i.e. the number of hysteretic units in state 1 at extreme values of the drive parameter *x*), and N_0 for the number of units in state 1 at the start of the protocol (usually in the rest state). Considering the strain as driving parameter we then obtain:

$$\left[d\sigma\right]_{\varepsilon_A\to\varepsilon_B} = \int_{\varepsilon_A}^{\varepsilon_B} K_{EU}(\varepsilon)d\varepsilon + K_0\frac{\gamma}{N_\infty - N_0}\left[\iint_{\Omega_B}\rho_\varepsilon\left(\varepsilon_0,\varepsilon_1\right)d\varepsilon_1 d\varepsilon_0 - \iint_{\Omega_A}\rho_\varepsilon\left(\varepsilon_0,\varepsilon_1\right)d\varepsilon_1 d\varepsilon_0\right] \qquad (3)$$

The contribution thus generally consists of a classical nonlinear part and a hysteretic part. Here, the double integrals are calculated over the 2D areas Ω_j in the PM space covering the hysteretic units which are in state 1 at the drive parameter ε_j, given the past history of $\varepsilon(t)$. It is exactly this history dependence that is responsible for the appearance of hysteresis in the quasi-static stress-strain relation, hysteresis and discontinuities in the modulus-strain relation, and effects such as end-point memory.

After renormalisation, and explicit introduction of a series expansion for $K_{EU}(\varepsilon)$:

$$\begin{aligned}\left[d\sigma\right]_{\varepsilon_A\to\varepsilon_B} &= \left[d\sigma_{ClassNL}\right]_{\varepsilon_A\to\varepsilon_B} + \left[d\sigma_{Hyst}\right]_{\varepsilon_A\to\varepsilon_B} \\ &= K_0\left(\int_{\varepsilon_A}^{\varepsilon_B}(1+2\beta\varepsilon+3\delta\varepsilon^2+...)d\varepsilon + \left[\iint_{\Omega_B}\tilde{\rho}_\varepsilon\left(\varepsilon_0,\varepsilon_1\right)d\varepsilon_1 d\varepsilon_0 - \iint_{\Omega_A}\tilde{\rho}_\varepsilon\left(\varepsilon_0,\varepsilon_1\right)d\varepsilon_1 d\varepsilon_0\right]\right)\end{aligned} \qquad (4)$$

A strong advantage of the PM model is that it can be implemented and used for arbitrary protocols. Besides, even though the model is phenomenological, several studies have shown that there is evidence of physical mechanisms that support the framework [43-49]. Examples of particular macroscopic features in the wave propagation for hysteretic materials have been considered in many earlier publications [6-12,17-23,50].

Apart from the property of end-point memory, a PM system has an additional important property that is related to the drive parameter. Internal loops between two identical drive parameter values on any increasing or decreasing branch of the stress-strain relation, should be congruent. The congruency also implies (in the limit of infinitesimal internal loops) that the value of the dynamic modulus as function of the drive parameter is independent of the history of the drive parameter, i.e. identical for increasing or decreasing branches. Experimental work on rocks, probing the wavespeed of longitudinal waves during uniaxial quasi static loading, has shown that hysteresis persists in the velocity versus stress, whereas it vanishes when plotting the velocity versus strain. An example is

shown in Figure 1 for Serena Sandstone. Based on similar experiments conducted on a large variety of rocks, all supporting the above observation, we conclude that it is more appropriate to use the strain-strain PM space formalism than the stress-stress PM space.

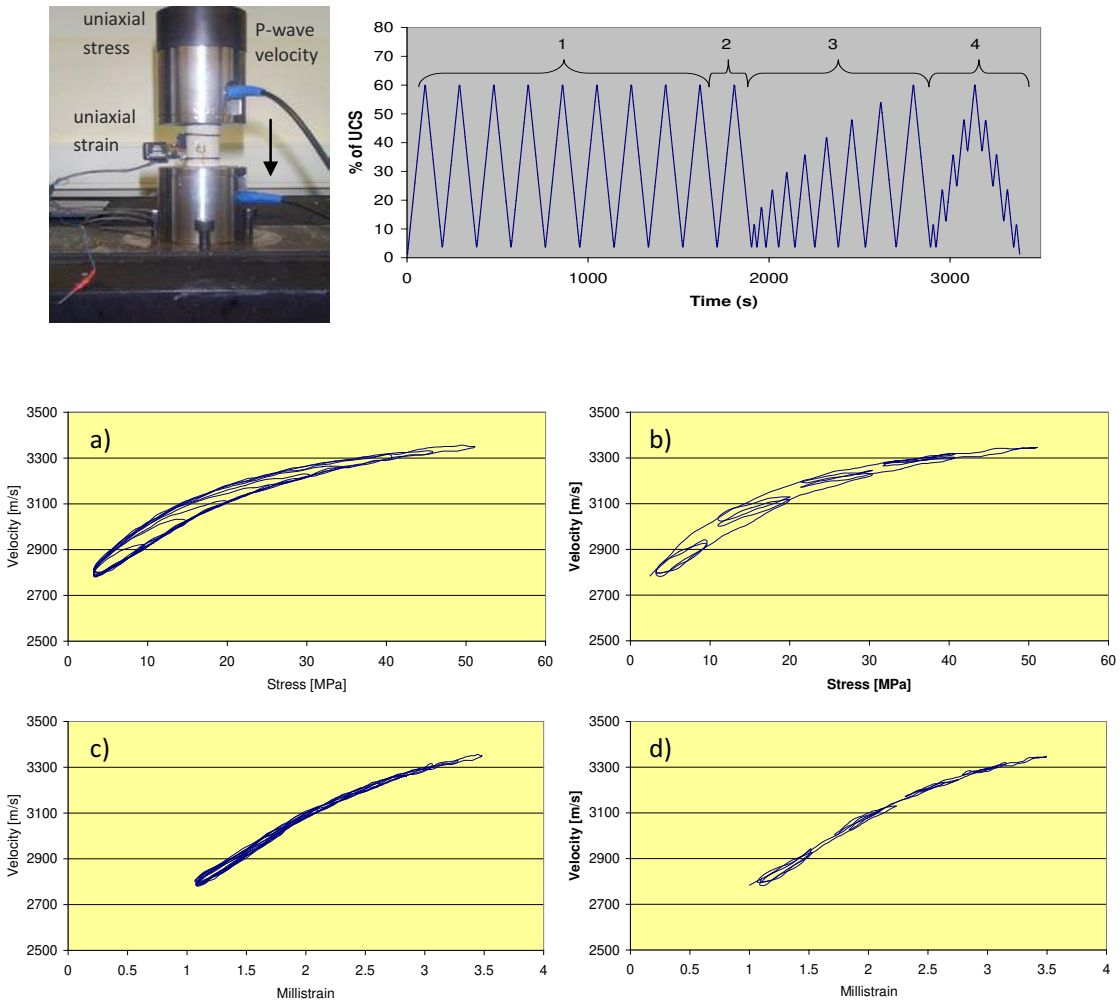

Figure 1: Acousto-elastic effect showing the path-dependence of wavespeed versus stress and versus strain during uniaxial compression experiments. Top: experimental set-up and typical protocol used in the experiments identifying 4 subsections. Bottom: a) wavespeed versus applied stress for subsection 3; b) wavespeed versus applied stress for subsection 4; c) wavespeed versus induced strain for subsection 3; d) wavespeed versus induced strain for subsection 4.

As mentioned above, the PM space formalism can be used for arbitrary protocols. In many cases when continuous monofrequency drives are considered (as in long burst propagation, or discrete step resonance experiments), the drive parameter basically oscillates between two values, symmetric with respect to zero, without any intermediate maxima or minima. If we call $\Delta\varepsilon$ the amplitude of the oscillation, then the excitation consists of an alternating sequence of a monotonically increasing branch from $-\Delta\varepsilon$ to $\Delta\varepsilon$, and a monotonically decreasing branch from $\Delta\varepsilon$ to-$-\Delta\varepsilon$. The PM-space formalism allows us to easily calculate the corresponding stress-strain relations for any given density. We call $\sigma^{+}(\varepsilon)$ the "upgoing" stress branch corresponding to the increasing strain, and $\sigma^{-}(\varepsilon)$ the "downgoing" stress corresponding to the decreasing strain. These two branches will be different if hysteresis is present (non-zero PM space density). Furthermore, due to the end-point memory property, the complete stress-strain loop will be closed.

If we assume cyclic excitation, and an initial situation (after rest) such that all hysteretic units with $\left|\varepsilon_0\right| \le -\varepsilon_1$ (i.e. below the anti-diagonal) are in state 1, we can deduce the following general expressions for the up- and downgoing branches of the stress-strain relation, assuming the contribution of the classical nonlinearity and the PM space density are known:

$$\begin{aligned}\sigma^{+}(\varepsilon) &= \sigma_{ClassNL}(\varepsilon) + \sigma^{+}_{Hyst}(\varepsilon) = \sigma_{ClassNL}(\varepsilon) + \left[\sigma_{Hyst}\right]_{-\Delta\varepsilon\to\varepsilon} \\ &= \sigma_{ClassNL}(\varepsilon) + K_0\left(\int_{-\Delta\varepsilon}^{0}\int_{\varepsilon_1}^{-\varepsilon_1}\tilde{\rho}_{\varepsilon}\left(\varepsilon_0,\varepsilon_1\right)d\varepsilon_0 d\varepsilon_1 - \int_{-\Delta\varepsilon}^{\varepsilon}\int_{-\Delta\varepsilon}^{\varepsilon_0}\tilde{\rho}_{\varepsilon}\left(\varepsilon_0,\varepsilon_1\right)d\varepsilon_1 d\varepsilon_0\right)\end{aligned} \tag{5}$$

$$\begin{aligned}\sigma^{-}(\varepsilon) &= \sigma_{ClassNL}(\varepsilon) + \sigma^{-}_{Hyst}(\varepsilon) = \sigma_{ClassNL}(\varepsilon) + \left[\sigma_{Hyst}\right]_{\Delta\varepsilon\to\varepsilon} \\ &= \sigma_{ClassNL}(\varepsilon) + K_0\left(-\int_{0}^{\Delta\varepsilon}\int_{-\varepsilon_0}^{\varepsilon_0}\tilde{\rho}_{\varepsilon}\left(\varepsilon_0,\varepsilon_1\right)d\varepsilon_1 d\varepsilon_0 + \int_{\varepsilon}^{\Delta\varepsilon}\int_{\varepsilon_1}^{\Delta\varepsilon}\tilde{\rho}_{\varepsilon}\left(\varepsilon_0,\varepsilon_1\right)d\varepsilon_0 d\varepsilon_1\right)\end{aligned} \tag{6}$$

Inversely, if the up- and downgoing curves are known (e.g. from experiments or -as assumed later- from simple analytic models), we can easily derive the associated PM space density, the classical nonlinearity contribution, the mean modulus change and the nonlinear attenuation.

The PM space density can be derived by considering the above expressions as functions of ε and $\Delta\varepsilon$ and by subtracting double derivatives of the up- and downgoing curves as follows:

$$\tilde{\rho}(\varepsilon_o,\varepsilon_c) = \frac{1}{2K_0}\left(\left[\frac{\partial}{\partial(-\Delta\varepsilon)}\left[\frac{\partial\sigma^{+}(\varepsilon,\Delta\varepsilon)}{\partial\varepsilon}\right]_{\varepsilon=\varepsilon_o}\right]_{(-\Delta\varepsilon)=\varepsilon_c} - \left[\frac{\partial}{\partial(\Delta\varepsilon)}\left[\frac{\partial\sigma^{-}(\varepsilon,\Delta\varepsilon)}{\partial\varepsilon}\right]_{\varepsilon=\varepsilon_c}\right]_{\Delta\varepsilon=\varepsilon_o}\right) \tag{7}$$

When the up- and downgoing curves are known and the density is calculated according to the above expression, we can also find the contribution of the classical nonlinearity as follows

$$\sigma_{ClassNL}(\varepsilon) = \sigma^{+}(\varepsilon) - \sigma^{+}_{Hyst}(\varepsilon)$$
$$= \sigma^{+}(\varepsilon) - K_0\left(\int_{-\Delta\varepsilon}^{0}\int_{\varepsilon_1}^{-\varepsilon_1}\tilde{\rho}_{\varepsilon}(\varepsilon_0,\varepsilon_1)d\varepsilon_0 d\varepsilon_1 - \int_{-\Delta\varepsilon}^{\varepsilon}\int_{-\Delta\varepsilon}^{\varepsilon_0}\tilde{\rho}_{\varepsilon}(\varepsilon_0,\varepsilon_1)d\varepsilon_1 d\varepsilon_0\right) \quad (8)$$

or equivalently by

$$\sigma_{ClassNL}(\varepsilon) = \sigma^{-}(\varepsilon) - \sigma^{-}_{Hyst}(\varepsilon)$$
$$= \sigma^{-}(\varepsilon) - K_0\left(-\int_{0}^{\Delta\varepsilon}\int_{-\varepsilon_0}^{\varepsilon_0}\tilde{\rho}_{\varepsilon}(\varepsilon_0,\varepsilon_1)d\varepsilon_1 d\varepsilon_0 + \int_{\varepsilon}^{\Delta\varepsilon}\int_{\varepsilon_1}^{\Delta\varepsilon}\tilde{\rho}_{\varepsilon}(\varepsilon_0,\varepsilon_1)d\varepsilon_0 d\varepsilon_1\right) \quad (9)$$

Under the above mentioned assumptions, we can calculate the mean modulus change during a full excursion. In the most general form, this can be expressed as:

$$\frac{K_0 - K}{K_0} = \frac{\Delta K}{K_0} = 1 - \frac{1}{K_0}\frac{\int_{-\Delta\varepsilon}^{\Delta\varepsilon}\frac{\partial\sigma^{+}}{\partial\varepsilon}d\varepsilon + \int_{-\Delta\varepsilon}^{\Delta\varepsilon}\frac{\partial\sigma^{-}}{\partial\varepsilon}d\varepsilon}{4\Delta\varepsilon} \quad (10)$$

Finally, the hysteretic losses (nonlinear attenuation) from the ratio of the loop area to the strain energy amount to:

$$\frac{1}{Q} - \frac{1}{Q_0} = \frac{\Delta\delta}{\pi} = \frac{1}{2\pi}\frac{\int_{-\Delta\varepsilon}^{\Delta\varepsilon}(\sigma^{+} - \sigma^{-})d\varepsilon}{\frac{1}{2}K_0(\Delta\varepsilon)^2} \quad (11)$$

Read introduced the ratio of nonlinear attenuation to mean modulus change as the "Read" parameter [22,23], expressing the relative importance of nonlinear attenuation over nonlinear elasticity. In general this yield:

$$R = \frac{\Delta\delta}{\frac{K_0 - K}{K_0}} = \frac{\frac{4}{\Delta\varepsilon}\int_{-\Delta\varepsilon}^{\Delta\varepsilon}(\sigma^{+} - \sigma^{-})d\varepsilon}{4K_0\Delta\varepsilon - \int_{-\Delta\varepsilon}^{\Delta\varepsilon}\frac{\partial\sigma^{+}}{\partial\varepsilon}d\varepsilon + \int_{-\Delta\varepsilon}^{\Delta\varepsilon}\frac{\partial\sigma^{-}}{\partial\varepsilon}d\varepsilon} \quad (12)$$

The read parameter has been calculated from experimental data by several people [3,6,18,21,24]. Typical values range between 0.3 and 3.

Using the generic PM-formalism, the Read parameter can be calculated for any type of PM density distribution, following equations (5-12). As we will illustrate further, the theoretical value of the Read parameter is a constant only for particular density distributions (e.g. for powerlaw dependence of

the density away from the diagonal in the PM space), and will not be constant at all with amplitude for general distributions.

2. Quadratic nonlinear hysteretic model.

The most inconvenient disadvantage about the general PM-space formalism is that there are too many free parameters by which the density can be described. Any function can be used for the density. Likewise, for the inversion of the PM-space density from experimental data, a discretisation of the drive parameter range into N intervals, leads to N(N+1)/2 degrees of freedom for the PM-space. This is for most cases impractical. A more workable manner, which can be especially helpful for dynamic wave propagation (small but finite amplitude), is to assume a formal expression for the density using a low number of parameters. For example, McCall et al. [14] and Van Den Abeele et al.[20] have deduced closed form expressions for the upgoing and downgoing branches of the stress-strain loops when the density of the PM-space is constant, say "α", and when the drive parameter is simply oscillating with amplitude $\Delta\varepsilon$ (no intermediate extrema). In this case only one parameter determines the hysteretic contribution. Additional parameters (e.g. β and δ) may be introduced to account for the contribution of classical nonlinearity. The closed form expressions for a constant PM-density then read:

$$\begin{cases} \sigma^{+}(\varepsilon) = K_0\left(\varepsilon + \beta\varepsilon^2 + \delta\varepsilon^3 + \ldots - \alpha(\Delta\varepsilon)\varepsilon + \frac{\alpha}{2}\left((\Delta\varepsilon)^2 - \varepsilon^2\right)\right) \\ \sigma^{-}(\varepsilon) = K_0\left(\varepsilon + \beta\varepsilon^2 + \delta\varepsilon^3 + \ldots - \alpha(\Delta\varepsilon)\varepsilon - \frac{\alpha}{2}\left((\Delta\varepsilon)^2 - \varepsilon^2\right)\right) \end{cases} \tag{13}$$

In the case when δ=0, and all higher order terms in the series expansion are neglected, the model is called the quadratic nonlinear hysteretic model. In this model

$$\begin{cases} \sigma^{+}(\varepsilon) = K_0\left(\varepsilon + \beta\varepsilon^2 + \alpha\left((\Delta\varepsilon)^2 - \frac{1}{2}(\Delta\varepsilon + \varepsilon)^2\right)\right) \\ \sigma^{-}(\varepsilon) = K_0\left(\varepsilon + \beta\varepsilon^2 - \alpha\left((\Delta\varepsilon)^2 - \frac{1}{2}(\Delta\varepsilon - \varepsilon)^2\right)\right) \end{cases} \tag{14}$$

In accordance to the general scheme discussed in Eqs. 7-8, assuming an initial situation (after rest) where all hysteretic units with $|\varepsilon_0| \le -\varepsilon_1$ (i.e. below the anti-diagonal) are in state 1, we can easily identify that:

$$\begin{cases} \tilde{\rho}_{\varepsilon}(\varepsilon_0, \varepsilon_1) = \alpha \\ \\ \sigma_{ClassNL}(\varepsilon) = K_0\left(\varepsilon + \beta\varepsilon^2\right) \end{cases} \tag{15}$$

Indeed, in a steady cyclic excitation between $-\Delta\varepsilon$ and $\Delta\varepsilon$, the PM space contribution to the upgoing stress-strain curve at a strain value ε will be

$$\begin{aligned} \sigma^{+}_{Hyst}(\varepsilon) = \left[\sigma_{Hyst}\right]_{-\Delta\varepsilon\to\varepsilon} &= K_0\left(\int_{-\Delta\varepsilon}^{0}\int_{\varepsilon_1}^{-\varepsilon_1}\tilde{\rho}_{\varepsilon}\left(\varepsilon_0,\varepsilon_1\right)d\varepsilon_0 d\varepsilon_1 - \int_{-\Delta\varepsilon}^{\varepsilon}\int_{-\Delta\varepsilon}^{\varepsilon_0}\tilde{\rho}_{\varepsilon}\left(\varepsilon_0,\varepsilon_1\right)d\varepsilon_1 d\varepsilon_0\right) \\ &= K_0\alpha\left((\Delta\varepsilon)^2 - \frac{1}{2}(\Delta\varepsilon+\varepsilon)^2\right) \end{aligned} \tag{16}$$

Likewise, the PM space contribution to the downgoing stress-strain curve at a strain value ε will be

$$\begin{aligned} \sigma^{-}_{Hyst}(\varepsilon) = \left[\sigma_{Hyst}\right]_{\Delta\varepsilon\to\varepsilon} &= K_0\left(-\int_{0}^{\Delta\varepsilon}\int_{-\varepsilon_0}^{\varepsilon_0}\tilde{\rho}_{\varepsilon}\left(\varepsilon_0,\varepsilon_1\right)d\varepsilon_1 d\varepsilon_0 + \int_{\varepsilon}^{\Delta\varepsilon}\int_{\varepsilon_1}^{\Delta\varepsilon}\tilde{\rho}_{\varepsilon}\left(\varepsilon_0,\varepsilon_1\right)d\varepsilon_0 d\varepsilon_1\right) \\ &= -K_0\alpha\left((\Delta\varepsilon)^2 - \frac{1}{2}(\Delta\varepsilon-\varepsilon)^2\right) \end{aligned} \tag{17}$$

The curve connecting the maxima and minima of the stress-strain loops for increasing excursion amplitudes $\Delta\varepsilon$, also called the 'initial' curve, is:

$$\sigma_{Init}(\Delta\varepsilon) = K_0\left(\Delta\varepsilon + \beta(\Delta\varepsilon)^2 - sign(\dot{\varepsilon})\alpha(\Delta\varepsilon)^2\right) \tag{18}$$

with *sign*(*x*)=1 if *x*>0 and -1 if *x*<0. The curve corresponds to the trajectory that is followed each time the absolute value of the excitation strain is exceeding the maximum absolute value of the strain within the preceding time history of the strain. Thus, starting from a situation at rest, the initial curve is followed until a certain maximum or minimum is reached, say at ε_1. When the strain rate changes sign, the stress-strain curve corresponds to an up- or downgoing curve (cfr Eq. 13) until $|\varepsilon| > |\varepsilon_1|$. For the particular 'initial' curve expressed by Eq.18, and assuming cyclic excursions with amplitudes $\Delta\varepsilon$, the tangent of the upgoing branch equals the tangent of σ_{Init} at $\Delta\varepsilon$. At the same time, the tangent of the downgoing branch equals the tangent of σ_{Init} at $-\Delta\varepsilon$. This assures end-point memory for any protocol.

From Eq.(14), an expression for the modulus can be deduced, which can be written in the following form:

$$K(\varepsilon) = K_0\left(1 + 2\beta\varepsilon - \alpha(\Delta\varepsilon + \mathrm{s}\,ign(\dot{\varepsilon})\varepsilon)\right). \tag{19}$$

This is a typical butterfly behavior as function of the strain, which is slanted when $\beta \neq 0$. In this model, the mean modulus relative change (cfr Eq.10), which is the quantity that can be derived from a standard resonance experiment, is $\alpha \Delta\varepsilon$, whereas the nonlinear attenuation (cfr Eq.11) amounts to $\frac{4\alpha \Delta\varepsilon}{3}$, yielding a Read parameter of $\frac{4}{3}$.

Typical results of the quadratic hysteretic model are illustrated in Figure 2.

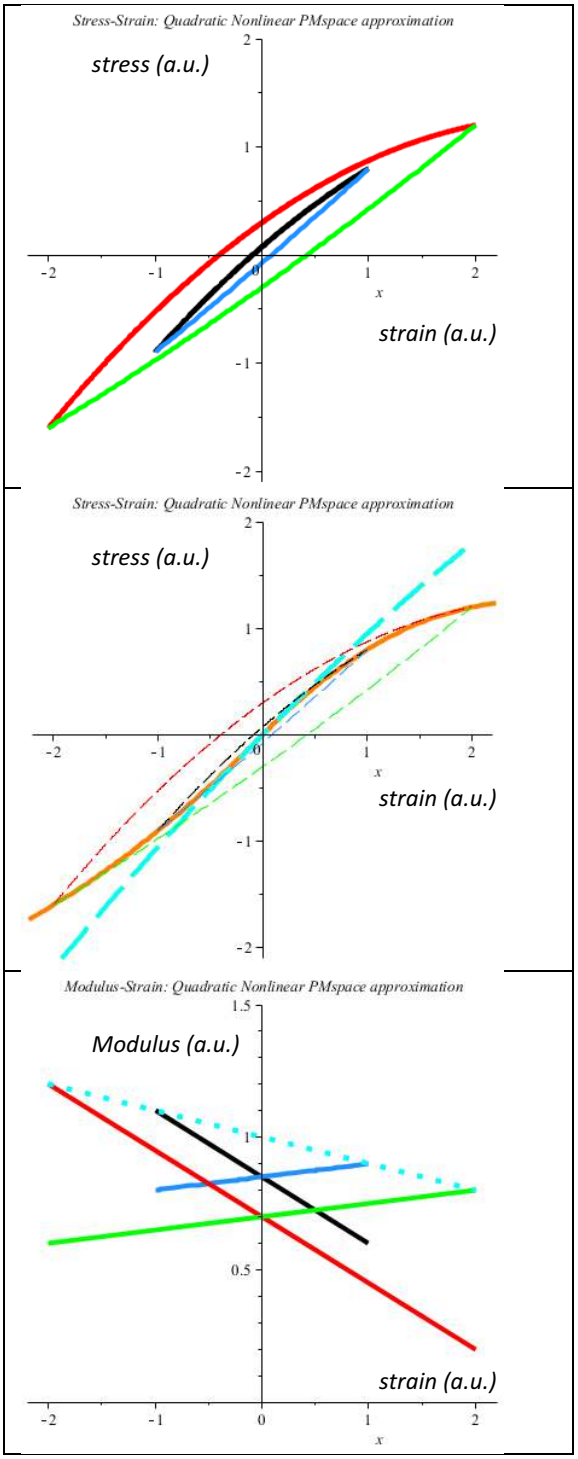

Figure 2: The quadratic nonlinear hysteretic model (Eq.(13), with $K_0 = 1; \beta = -0.05; \alpha = 0.15$):
a) stress-strain curves for two amplitudes (low amplitude: black-blue; high amplitude: red-green); b) Initial curve (orange, Eq.18) and classical nonlinear stress-strain contribution (dashed cyan, Eq. 15b) on top of the stress-strain curves; c) Modulus-strain curves for two amplitudes (Eq. 19) and classical nonlinear modulus-strain contribution (dotted cyan).

3. Adapted quadratic model of Nazarov et al.

A variation on the closed form expressions presented in Eq.13 was proposed by Nazarov et al. [12], who proposed the following form:

$$\begin{cases} \sigma^{+}(\varepsilon) = K_0\left(\varepsilon - \alpha(\Delta\varepsilon)\varepsilon + \left(\frac{\beta_1+\beta_2}{4}(\Delta\varepsilon)^2 - \frac{\beta_1}{2}\varepsilon^2\right)\right) \\ \sigma^{-}(\varepsilon) = K_0\left(\varepsilon - \alpha(\Delta\varepsilon)\varepsilon - \left(\frac{\beta_1+\beta_2}{4}(\Delta\varepsilon)^2 - \frac{\beta_2}{2}\varepsilon^2\right)\right) \end{cases} \tag{20}$$

Compared to Eq.13, the original (classical nonlinear) parameters β and δ are set to zero, whereas the nonlinear terms in the state relation are quadratic in nature and described by three parameters: α, β_1 and β_2. Note that

- if $\beta_1 = \beta_2 = \alpha$, the model of Nazarov is exactly the same as the above discussed quadratic nonlinear hysteretic model, without the quadratic term in the classical nonlinearity contribution.
- if $\beta_1 = \beta_2 = 0$, the model of Nazarov is a nonlinear model without hysteresis. The up- and downgoing loops are identical but the slope (modulus) reduces with increasing excitation amplitude: $\sigma^{+}(\varepsilon) = \sigma^{-}(\varepsilon) = K_0\left(1 - \alpha(\Delta\varepsilon)\right)\varepsilon$. Thus there is no hysteresis in the system, nevertheless, the system has memory, in particular related to its largest level of excitation.

The model of Nazarov can be rewritten in the following form (in accordance to Eq. 14) which makes it easier to identify the classical nonlinear term, the hysteretic term and an additional non-hysteretic but memory dependent term:

$$\begin{cases} \sigma^{+}(\varepsilon) = K_0\left(\varepsilon - \frac{\beta_1-\beta_2}{4}\varepsilon^2 - (\alpha - \frac{\beta_1+\beta_2}{2})(\Delta\varepsilon)\varepsilon + \frac{\beta_1+\beta_2}{2}\left((\Delta\varepsilon)^2 - \frac{1}{2}(\Delta\varepsilon+\varepsilon)^2\right)\right) \\ \sigma^{-}(\varepsilon) = K_0\left(\varepsilon - \frac{\beta_1-\beta_2}{4}\varepsilon^2 - (\alpha - \frac{\beta_1+\beta_2}{2})(\Delta\varepsilon)\varepsilon - \frac{\beta_1+\beta_2}{2}\left((\Delta\varepsilon)^2 - \frac{1}{2}(\Delta\varepsilon-\varepsilon)^2\right)\right) \end{cases} \tag{21}$$

Due to the non-hysteretic memory term in this expression, this model can not correspond to a true PM-space. Still, using a superposition of contributions such as:

$$\begin{cases} \sigma^{+}(\varepsilon) = \sigma_{ClassNL}(\varepsilon) + \sigma_{MemoryNL}(\varepsilon,\Delta\varepsilon) + \sigma^{+}_{Hyst}(\varepsilon) \\ \qquad = \sigma_{ClassNL}(\varepsilon) + \sigma_{MemoryNL}(\varepsilon,\Delta\varepsilon) + K_0\left(\int_{-\Delta\varepsilon}^{0}\int_{\varepsilon_1}^{-\varepsilon_1} \tilde{\rho}_{\varepsilon}(\varepsilon_0,\varepsilon_1)\,d\varepsilon_0 d\varepsilon_1 - \int_{-\Delta\varepsilon}^{\varepsilon}\int_{-\Delta\varepsilon}^{\varepsilon_0} \tilde{\rho}_{\varepsilon}(\varepsilon_0,\varepsilon_1)\,d\varepsilon_1 d\varepsilon_0 \right) \\ \sigma^{-}(\varepsilon) = \sigma_{ClassNL}(\varepsilon) + \sigma_{MemoryNL}(\varepsilon,\Delta\varepsilon) + \sigma^{-}_{Hyst}(\varepsilon) \\ \qquad = \sigma_{ClassNL}(\varepsilon) + \sigma_{MemoryNL}(\varepsilon,\Delta\varepsilon) + K_0\left(-\int_{0}^{\Delta\varepsilon}\int_{-\varepsilon_0}^{\varepsilon_0} \tilde{\rho}_{\varepsilon}(\varepsilon_0,\varepsilon_1)\,d\varepsilon_1 d\varepsilon_0 + \int_{\varepsilon}^{\Delta\varepsilon}\int_{\varepsilon_1}^{\Delta\varepsilon} \tilde{\rho}_{\varepsilon}(\varepsilon_0,\varepsilon_1)\,d\varepsilon_0 d\varepsilon_1 \right) \end{cases} \tag{22}$$

we can identify that:

$$\begin{cases} \sigma_{ClassNL}(\varepsilon) = K_0\left(\varepsilon - \dfrac{\beta_1-\beta_2}{4}\varepsilon^2 \right) \\ \sigma_{MemoryNL}(\varepsilon,\Delta\varepsilon) = -K_0\left(\alpha - \dfrac{\beta_1+\beta_2}{2} \right)(\Delta\varepsilon)\varepsilon \\ \tilde{\rho}_{\varepsilon}(\varepsilon_0,\varepsilon_1) = \dfrac{\beta_1+\beta_2}{2} \end{cases} \tag{23}$$

The "initial curve" (as defined above) in this case is

$$\sigma_{Init}(\Delta\varepsilon) = K_0\left(\Delta\varepsilon - \frac{\beta_1-\beta_2}{4}(\Delta\varepsilon)^2 - sign(\dot{\varepsilon})\,\alpha(\Delta\varepsilon)^2 \right) \tag{24}$$

while the modulus reads:

$$\begin{aligned} K^{+}(\varepsilon) &= K_0\left(1-\beta_1\varepsilon-\alpha\,\Delta\varepsilon\right) \\ K^{-}(\varepsilon) &= K_0\left(1+\beta_2\varepsilon-\alpha\,\Delta\varepsilon\right) \end{aligned}. \tag{25}$$

The mean modulus relative change is again $\alpha\,\Delta\varepsilon$. The nonlinear attenuation originating from the hysteresis loop is $\frac{2(\beta_1+\beta_2)\,\Delta\varepsilon}{3}$. This provides a Read parameter of $\frac{2}{3}\frac{(\beta_1+\beta_2)}{\alpha}$.

Note that for the model of Nazarov:

- The Read parameter is larger than 4/3 when $\beta_1+\beta_2 > 2\alpha$ and smaller than 4/3 when $\beta_1+\beta_2 < 2\alpha$. It can take any value between 0 (for $\beta_1=\beta_2=0$) and infinity (for $\alpha=0$).
- Strictly speaking the model can only be deduced from a PM-space model when $\beta_1+\beta_2=2\alpha$. In this case, the non-hysteretic memory term contributing to a reduction of the modulus is zero.

Illustrations of the adapted quadratic hysteretic model according to Nazarov can be found in Figure 3.

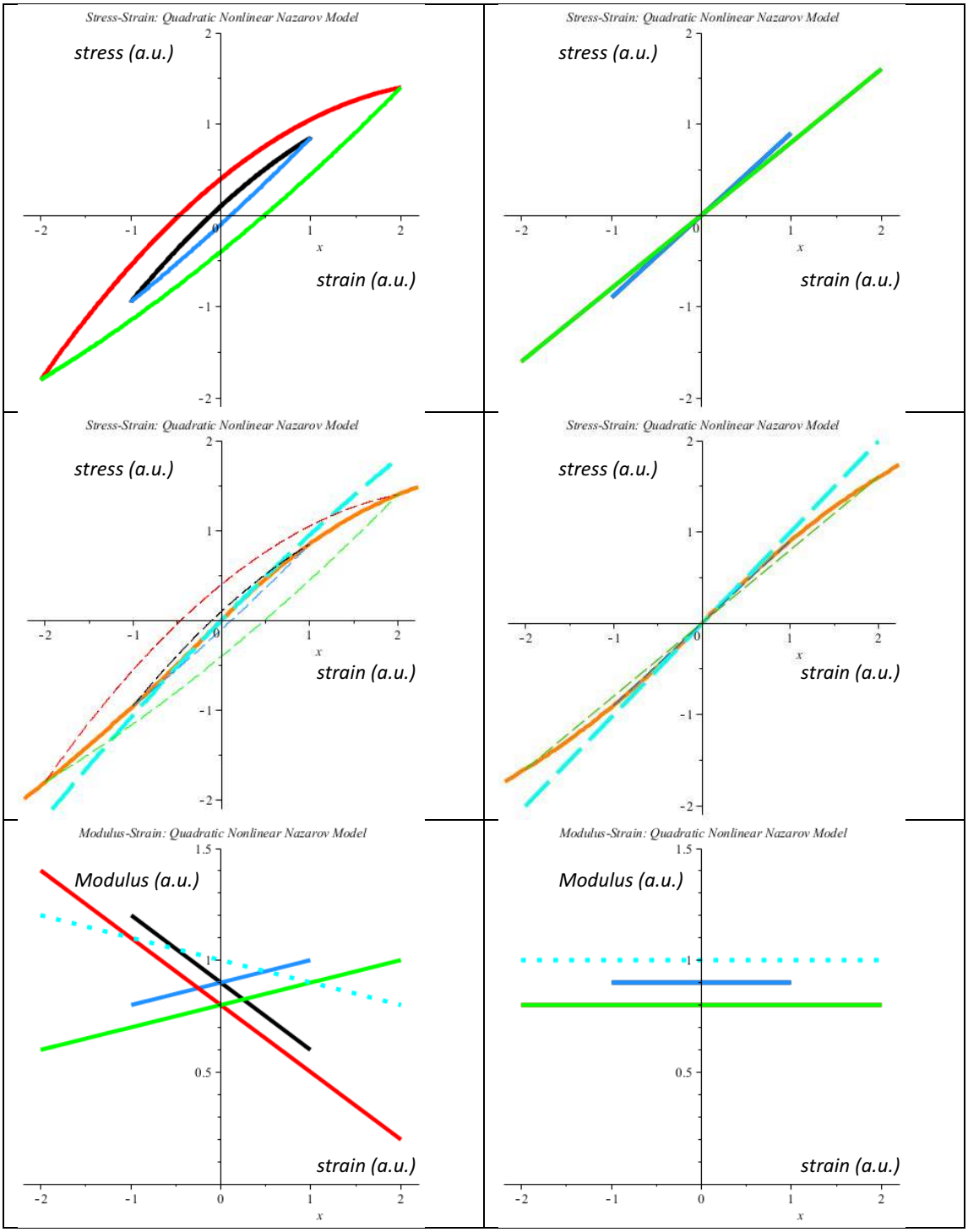

Figure 3: The adapted quadratic nonlinear model following Nazarov et al. (Eq.(15): Left hand side for $K_0 = 1; \alpha = 0.1; \beta_1 = 0.3; \beta_2 = 0.1$ (hysteretic case); Right hand side for $K_0 = 1; \alpha = 0.1; \beta_1 = 0.0; \beta_2 = 0.0$ (non-hysteretic case).

Top) stress-strain curves for two amplitudes (low amplitude: black-blue; high amplitude: red-green); Middle) Initial curve (orange, Eq. 24) and classical nonlinear stress-strain contribution (dashed cyan, Eq. 23a) on top of the stress-strain curves; Bottom) Modulus-strain curves for two amplitudes (Eq. 25) and classical nonlinear modulus-strain contribution (dotted cyan).

4. The original and adapted model of Davidenkov et al.

The adapted Davidenkov model [2,3,12] assumes the following expressions for the stress-strain curves:

$$\begin{cases} \sigma^{+}(\varepsilon) = K_0\left(\varepsilon + \dfrac{\alpha}{m}\left(2^{m-1}(\Delta\varepsilon)^m - (\Delta\varepsilon+\varepsilon)^m\right)\right) \\ \sigma^{-}(\varepsilon) = K_0\left(\varepsilon - \dfrac{\alpha}{m}\left(2^{m-1}(\Delta\varepsilon)^m - (\Delta\varepsilon-\varepsilon)^m\right)\right) \end{cases} \tag{26}$$

It contains two parameters: α and *m*. The original model corresponds to the case when *m=2*, and thus coincides with the quadratic nonlinear hysteretic model discussed above (without contribution from classical nonlinearity).

Even though the model is introduced only for cyclic excitation, it is instructive to investigate the nature of the PM-space that might be associated with these equations, especially for *m>2*.

If we again assume as initial situation (after rest) that all hysteretic units with $|\varepsilon_0| \le -\varepsilon_1$ (i.e. below the anti-diagonal) are in state 1, and apply the derivation discussed in Eqs. 7 to 9, we obtain that:

$$\begin{cases} \tilde{\rho}_{\varepsilon}(\varepsilon_0, \varepsilon_1) = \alpha\ (m-1)\left(\varepsilon_0 - \varepsilon_1\right)^{m-2} \\ \\ \sigma_{ClassNL}(\varepsilon) = K_0\varepsilon \end{cases} \tag{27}$$

Note that the density is indeed constant (and equal to α) when *m=2*, as in the quadratic nonlinear hysteretic model. For m≠2, the density assumes a powerlaw relation with the argument being the distance from the diagonal in the PM-space. For *m=3* for instance, we obtain a linear increase of the density distribution away from the diagonal, etc. Finally, it should be mentioned that *m* should be larger than unity, since otherwise the PM density becomes negative for any positive value of α.

The "initial curve" connecting the maxima and minima of the stress-strain loops for increasing excursion amplitudes $\Delta\varepsilon$, in this case is

$$\sigma_{Init}(\Delta\varepsilon) = K_0\left(\Delta\varepsilon - \frac{\alpha}{m}(sign(\dot{\varepsilon})\cdot 2)^{m-1}\ (\Delta\varepsilon)^m\right) \tag{28}$$

Starting from Eq. 26, a simple expression for the modulus can be derived:

$$K(\varepsilon) = K_0\left(1 - \alpha\ (\Delta\varepsilon + sign(\dot{\varepsilon})\varepsilon)^{m-1}\right) \tag{29}$$

and results in $\frac{\Delta K}{K_0} = \frac{\alpha\, 2^{m-1}(\Delta\varepsilon)^{m-1}}{m}$ for the mean modulus relative change. The losses ($\Delta\delta$) due to the hysteresis are $\frac{2^{m-1}\alpha\,(m-1)\,(\Delta\varepsilon)^{m-1}}{3\,(m+1)}$. The ratio of these two quantities gives rise to a Read parameter of $\frac{4(m-1)}{(m+1)}$.

Note that for the (adapted) model of Davidenkov:

- The Read parameter can vary between 0 (for *m=1*, no nonlinearity at all) and 4 (for *m* large), with the above mentioned value of 4/3 for the quadratic case (*m=2*).
- In the special case when *m=1*, the system performs linearly, independent on the amplitude, with a modulus equal to $K_0\left(1-\alpha\right)$.

As mentioned above, the Davidenkov model corresponds to a PM-space density that is uniformly changing away from the diagonal according to a single powerlaw relation for the quantity $\left(\varepsilon_0-\varepsilon_1\right)$ (cfr Eq. 27). As an extension, one could equally well assume a more complicated density distribution, which is still a function of $\left(\varepsilon_0-\varepsilon_1\right)$, and approximate this distribution by means of a truncated Taylor series:

$$\tilde{\rho}_\varepsilon(\varepsilon_0,\varepsilon_1) = f\left(\varepsilon_0-\varepsilon_1\right) \approx \sum_{m=2}^{M} \alpha_m\,(m-1)\left(\varepsilon_0-\varepsilon_1\right)^{m-2} \tag{30}$$

with $\alpha_m\,(m-1) = \frac{1}{(m-2)!}\left[\frac{d^{m-2} f\left(x\right)}{d\,x^{m-2}}\right]_{x=0}$ for *m=2..M*.

As a result of the superposition of integer exponent powerlaws within the Taylor expansion, the corresponding up- and downgoing stress-strain curves in this case can also be written as a superposition of individual hysteretic contributions with integer exponents as introduced in Eq. 26, yielding

$$\begin{cases} \sigma^{+}(\varepsilon) = K_0\left(\varepsilon + \sum_{m=2}^{M} \frac{\alpha_m}{m}\left(2^{m-1}(\Delta\varepsilon)^m - (\Delta\varepsilon+\varepsilon)^m\right)\right) \\ \sigma^{-}(\varepsilon) = K_0\left(\varepsilon - \sum_{m=2}^{M} \frac{\alpha_m}{m}\left(2^{m-1}(\Delta\varepsilon)^m - (\Delta\varepsilon-\varepsilon)^m\right)\right) \end{cases} \tag{31}$$

Similarly, we can simply rewrite the initial curve and the modulus-strain relation as a superposition. The Read parameter, however, becomes more complicated due to the superposition of contributions with different exponents. The general expression clearly illustrates that the Read parameter may not longer be a constant any more. On the contrary, as soon as more than one power is involved, the ratio between losses and elasticity reduction becomes amplitude dependent:

$$R = \frac{\sum_{m=2}^{M} \frac{2^{m-1}\alpha_m (m-1)(\Delta\varepsilon)^{m-1}}{3(m+1)}}{\sum_{m=2}^{M} \frac{\alpha_m 2^{m-1}(\Delta\varepsilon)^{m-1}}{m}} \tag{32}$$

Typical results of the original and the extended Davidenkov model are displayed in Figure 4.

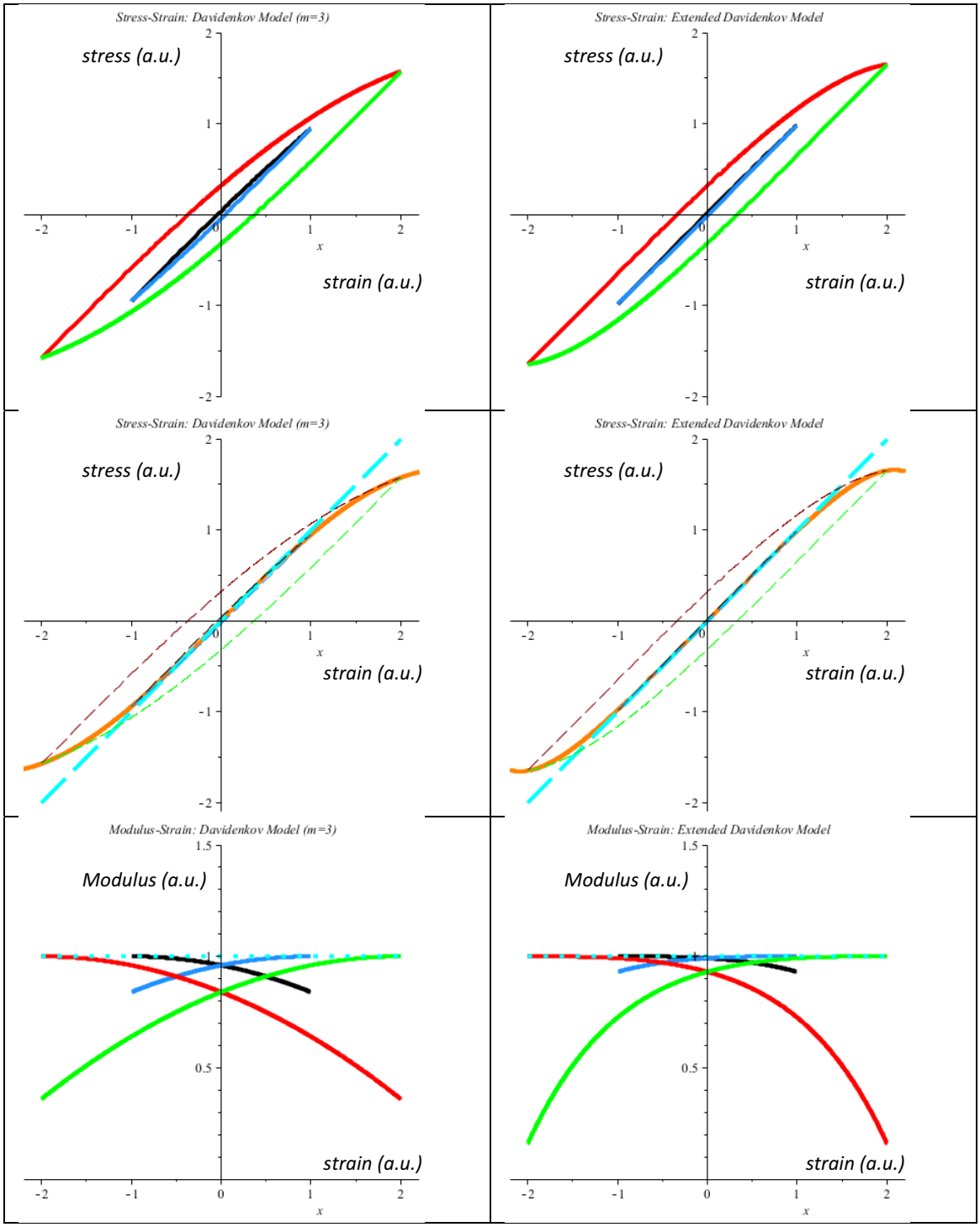

Figure 4: The original and extended Davidenkov model (Left hand side: Eq.(26) with $K_0 = 1; m = 3; \alpha = 0.04$; Right hand side Eq.(31) with $K_0 = 1; \alpha_4 = 0.008; \alpha_7 = 0.00008$.

Top) stress-strain curves for two amplitudes (low amplitude: black-blue; high amplitude: red-green); Middle) Initial curve (orange) and classical nonlinear stress-strain contribution (dashed cyan) on top of the stress-strain curves; Bottom) Modulus-strain curves for two amplitudes and classical nonlinear modulus-strain contribution (dotted cyan).

5. The (adapted) Granato-Lücke model

The stress-strain curves according to the (adapted) Granato-Lücke model contains four branches, and can be expressed as follows [5,6,12]:

$$\sigma(\varepsilon)=\begin{cases} K_0^+(\varepsilon-\dfrac{\gamma_1}{m}\varepsilon^m) & if \quad \varepsilon\geq 0,\dot{\varepsilon}\geq 0 \\ K_0^+(\varepsilon+\dfrac{\gamma_2}{m}\varepsilon^m-\dfrac{\gamma_1+\gamma_2}{m}(\Delta\varepsilon)^{m-1}\varepsilon) & if \quad \varepsilon\geq 0,\dot{\varepsilon}\leq 0 \\ K_0^-(\varepsilon+\dfrac{\gamma_3}{n}\left|\varepsilon\right|^n) & if \quad \varepsilon\leq 0,\dot{\varepsilon}\leq 0 \\ K_0^-(\varepsilon-\dfrac{\gamma_4}{n}\left|\varepsilon\right|^n-\dfrac{\gamma_3+\gamma_4}{n}(\Delta\varepsilon)^{n-1}\varepsilon) & if \quad \varepsilon\leq 0,\dot{\varepsilon}\geq 0 \end{cases} \tag{33}$$

Apart from the possibility to account for different moduli in tension and compression (K_0^+ and K_0^-), the model contains four nonlinear parameters and two exponents: $\gamma_1,\gamma_2,\gamma_3,\gamma_4$ and *m* and *n*. The original model corresponds to the case when *m=n=2*, and when $\gamma_2=\gamma_4=0$. In the case when $\gamma_1=-\gamma_2$, together with $\gamma_3=-\gamma_4$, the system is not hysteretic anymore and act as a classical nonlinear system with a possible discontinuity in the modulus-strain relation at the origin.

We again investigate the nature of the PM-space that might be associated with these equations. Remark that the stress-strain loops always go through the origin at zero strain. Independent of the protocol that was followed, the system assumes zero stress when the strain is zero. This property implies that the PM-space should be empty in the quadrant defined by $\varepsilon_0\geq 0$ and $\varepsilon_1\leq 0$. Furthermore, the initial state corresponds to the situation when all units in the triangle $\varepsilon_1\leq\varepsilon_0\leq 0$ are in state 1, and the units in the triangle $\varepsilon_0\geq\varepsilon_1\geq 0$ are in state 0. This observation really helps in finding the classical nonlinear contribution and the PM density associated with the Granato-Lücke model since it allows us to perform the calculations separately for loops in the $\varepsilon\geq 0$ quadrant and in the $\varepsilon\leq 0$ quadrant.

After some tedious calculations, we find that

$$\begin{cases} \sigma_{ClassNL}(\varepsilon)=K_0^+\left(\varepsilon+\left(\dfrac{\gamma_2}{m}-\dfrac{\gamma_1+\gamma_2}{m^2}\right)\varepsilon^m\right) & for \quad \varepsilon\geq 0 \\ \tilde{\rho}_\varepsilon(\varepsilon_0,\varepsilon_1)=\dfrac{\gamma_1+\gamma_2}{m}(m-1)\left(\varepsilon_0\right)^{m-2} & for \quad \varepsilon_0\geq\varepsilon_1\geq 0 \end{cases} \tag{34}$$

$$\begin{cases} \sigma_{ClassNL}(\varepsilon) = K_0^- \left(\varepsilon - \left(\dfrac{\gamma_4}{n} - \dfrac{\gamma_3+\gamma_4}{n^2} \right) |\varepsilon|^n \right) & for \quad \varepsilon \le 0 \\ \tilde{\rho}_\varepsilon(\varepsilon_0, \varepsilon_1) = \dfrac{\gamma_3+\gamma_4}{n}(n-1)\,|\varepsilon_1|^{n-2} & for \quad \varepsilon_1 \le \varepsilon_0 \le 0 \end{cases} \tag{35}$$

Note that the density within the upper and lower triangular areas is constant when *m=n=2*. For m≠2 and/or n≠2, the density assumes a powerlaw relation as function of the strain value ε_0 for $\varepsilon \ge 0$ and as function of ε_1 for $\varepsilon \le 0$. The powerlaw can be different in both cases. Again, it should be mentioned that both *m* and *n* should be larger than unity, since otherwise the PM density becomes negative for any positive values of $\gamma_1+\gamma_2$ and $\gamma_3+\gamma_4$.

The "initial curve" of the stress-strain loops is split in two curves, one connecting the maxima (found when $\varepsilon \ge 0$) and another connecting the minima, i.e. for $\varepsilon \le 0$:

$$\sigma_{Init}(\varepsilon) = \begin{cases} K_0^+ \left(\varepsilon - \dfrac{\gamma_1}{m}\varepsilon^m \right) & for \quad \varepsilon \ge 0 \\ K_0^- \left(\varepsilon + \dfrac{\gamma_3}{n}|\varepsilon|^n \right) & for \quad \varepsilon \le 0 \end{cases} \tag{36}$$

Note that the two pieces of the initial curve exactly correspond to branch 1 and 3 of the stress-strain expression given in Eq. (33).

Likewise, the mean modulus and the total hysteresis loop area over a full excursion are also composed of two parts ($\varepsilon \ge 0$ and $\varepsilon \le 0$), and amount respectively to

$$K_{mean}(\Delta\varepsilon) = \frac{K_0^+ \left(1 - \dfrac{\gamma_1}{m}(\Delta\varepsilon)^{m-1} \right) + K_0^- \left(1 - \dfrac{\gamma_3}{n}(\Delta\varepsilon)^{n-1} \right)}{2} \tag{37}$$

and

$$Area(\Delta\varepsilon) = K_0^+ \frac{(\gamma_1+\gamma_2)}{2m}\frac{m-1}{m+1}(\Delta\varepsilon)^{m-1} + K_0^- \frac{(\gamma_3+\gamma_4)}{2n}\frac{n-1}{n+1}(\Delta\varepsilon)^{n-1} \tag{38}$$

For equal values of the moduli in tension and compression (i.e. $K_0^+ = K_0^- = K_0$), and equal powerlaw exponents (i.e. *m=n*), the Read parameter becomes amplitude independent and yields:

$$R = \frac{(\gamma_1 + \gamma_2 + \gamma_3 + \gamma_4)}{(\gamma_1 + \gamma_3)} \frac{m-1}{m+1} \tag{39}$$

Note that for the original Granato-Lücke model (with *m=n=2*, and $\gamma_2 = \gamma_4 = 0$), the value of the R reduced to 1/3.

As in the Davidenkov model, we can extend the complexity by assuming a more general density distribution in both triangles, respectively $f^+(\varepsilon_0)$ and $f^-(|\varepsilon_1|)$, that can be approximated by means of a truncated Taylor series. If we assume

$$\begin{cases} \tilde{\rho}_\varepsilon(\varepsilon_0, \varepsilon_1) = f^+(\varepsilon_0) \approx \sum_{m=2}^{M} \frac{\gamma_{1,m} + \gamma_{2,m}}{m} (m-1) \left(\varepsilon_0\right)^{m-2} & for \quad \varepsilon_0 \geq \varepsilon_1 \geq 0 \\ \tilde{\rho}_\varepsilon(\varepsilon_0, \varepsilon_1) = f^-(|\varepsilon_1|) \approx \sum_{n=2}^{N} \frac{\gamma_{3,n} + \gamma_{4,n}}{n} (n-1) |\varepsilon_1|^{n-2} & for \quad \varepsilon_1 \leq \varepsilon_0 \leq 0 \end{cases} \tag{40}$$

with $\frac{\gamma_{1,m-2} + \gamma_{2,m-2}}{m} (m-1) = \frac{1}{(m-2)!} \left[\frac{d^{m-2} f^+(x)}{d\, x^{m-2}} \right]_{x=0}$ for *m=2..M*.

and $\frac{\gamma_{3,n-2} + \gamma_{4,n-2}}{n} (n-1) = \frac{1}{(n-2)!} \left[\frac{d^{n-2} f^-(x)}{d\, x^{n-2}} \right]_{x=0}$ for *n=2..N*

then the extended Granato-Lücke model can be written as:

$$\sigma(\varepsilon) = \begin{cases} K_0^+ (\varepsilon - \sum_{m=2}^{M} \frac{\gamma_{1,m}}{m} \varepsilon^m) & if \quad \varepsilon \geq 0, \dot{\varepsilon} \geq 0 \\ K_0^+ (\varepsilon + \sum_{m=2}^{M} \frac{\gamma_{2,m}}{m} \varepsilon^m - \sum_{m=2}^{M} \frac{\gamma_{1,m} + \gamma_{2,m}}{m} (\Delta\varepsilon)^{m-1} \varepsilon) & if \quad \varepsilon \geq 0, \dot{\varepsilon} \leq 0 \\ K_0^- (\varepsilon + \sum_{n=2}^{N} \frac{\gamma_{3,n}}{n} |\varepsilon|^n) & if \quad \varepsilon \leq 0, \dot{\varepsilon} \leq 0 \\ K_0^- (\varepsilon - \sum_{n=2}^{N} \frac{\gamma_{4,n}}{n} |\varepsilon|^n - \sum_{n=2}^{N} \frac{\gamma_{3,n} + \gamma_{4,n}}{n} (\Delta\varepsilon)^{n-1} \varepsilon) & if \quad \varepsilon \leq 0, \dot{\varepsilon} \geq 0 \end{cases} \tag{41}$$

with moduli given by

$$K(\varepsilon)=\begin{cases} K_0^+(1-\sum_{m=2}^{M}\gamma_{1,m}\varepsilon^{m-1}) & if \quad \varepsilon\geq 0,\dot{\varepsilon}\geq 0 \\ K_0^+(1+\sum_{m=2}^{M}\gamma_{2,m}\varepsilon^{m-1}-\sum_{m=2}^{M}\frac{\gamma_{1,m}+\gamma_{2,m}}{m}(\Delta\varepsilon)^{m-1}) & if \quad \varepsilon\geq 0,\dot{\varepsilon}\leq 0 \\ K_0^-(1-\sum_{n=2}^{N}\gamma_{3,n}\left|\varepsilon\right|^{n-1}) & if \quad \varepsilon\leq 0,\dot{\varepsilon}\leq 0 \\ K_0^-(1+\sum_{n=2}^{N}\gamma_{4,n}\left|\varepsilon\right|^{n-1}-\sum_{n=2}^{N}\frac{\gamma_{3,n}+\gamma_{4,n}}{n}(\Delta\varepsilon)^{n-1}) & if \quad \varepsilon\leq 0,\dot{\varepsilon}\geq 0 \end{cases} \tag{42}$$

As can be expected, the Read parameter becomes even more complicated in this case. After some routine calculations, we find, for $K_0^+=K_0^-=K_0$ and assuming *M=N*, that R reads:

$$R=\frac{\sum_{m=2}^{M}\frac{(\gamma_{1,m}+\gamma_{2,m}+\gamma_{3,m}+\gamma_{4,m})}{2m}\frac{m-1}{m+1}(\Delta\varepsilon)^{m-1}}{\sum_{m=2}^{M}\frac{(\gamma_{1,m}+\gamma_{3,m})}{2m}(\Delta\varepsilon)^{m-1}} \tag{43}$$

Similarly as for the extension of the Davidenkov model, the Read parameter results in a superposition of contributions with different exponents, and a general expression that clearly illustrates that the non-constant behavior of the Read parameter. The ratio between losses and elasticity reduction becomes amplitude dependent.

Illustrations of the original and the extended Granato-Lücke model can be found in Figures 5 and 6.

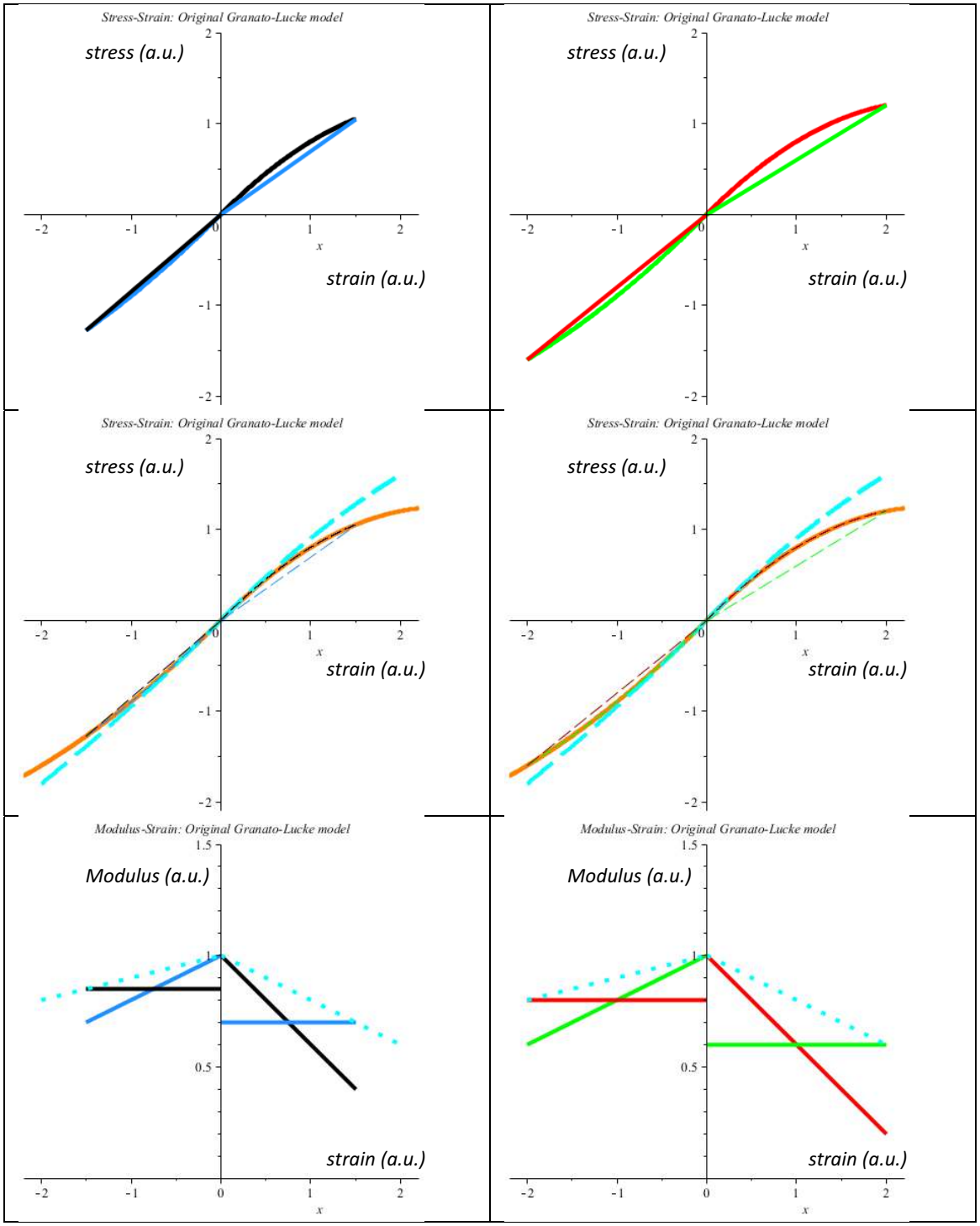

Figure 5: The original Granato-lücke model (Eq.(33) with $K_0^+ = K_0^- = 1; m = n = 2$; $\gamma_1 = 0.4; \gamma_2 = 0$; $\gamma_3 = 0.2; \gamma_4 = 0$) for two amplitudes (left, low amplitude: black-blue; right , high amplitude: red-green)

Top) stress-strain curves; Middle) Initial curve (orange) and classical nonlinear stress-strain contribution (dashed cyan) on top of the stress-strain curves; Bottom) Modulus-strain curves for two amplitudes and classical nonlinear modulus-strain contribution (dotted cyan).

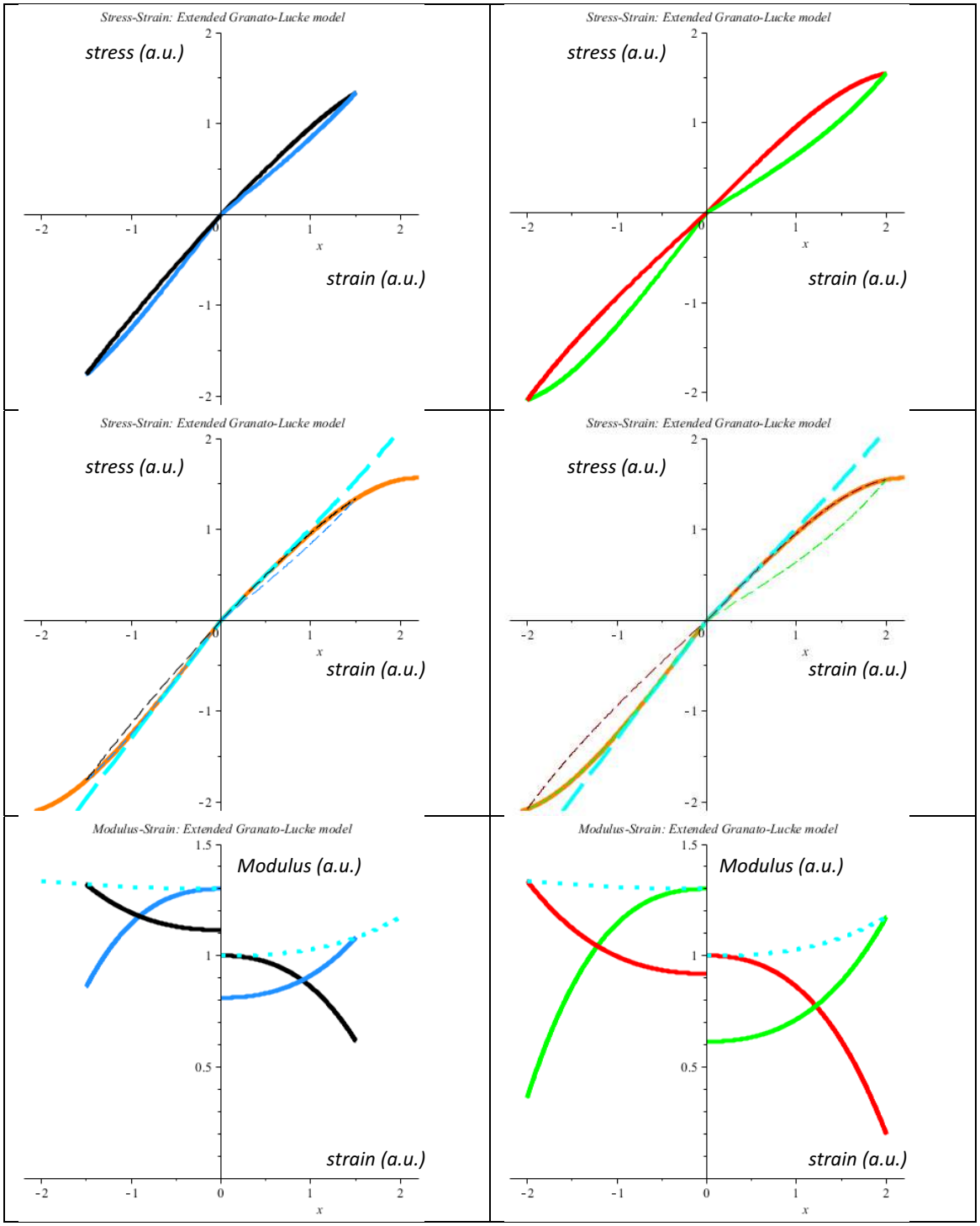

Figure 6: The extended Granato-lücke model (Eq.(41-42) with $K_0^+ = 1; K_0^- = 1.3$;
$\gamma_{1,3} = 0.08; \gamma_{2,3} = 0.06$; $\gamma_{3,3} = 0.06; \gamma_{4,3} = 0.04$; $\gamma_{1,4} = 0.06; \gamma_{2,4} = 0.04$; $\gamma_{3,4} = 0.06; \gamma_{4,4} = 0.02$)
for two amplitudes (left, low amplitude: black-blue; right , high amplitude: red-green)
Top) stress-strain curves; Middle) Initial curve (orange) and classical nonlinear stress-strain contribution (dashed cyan) on top of the stress-strain curves; Bottom) Modulus-strain curves for two amplitudes and classical nonlinear modulus-strain contribution (dotted cyan).

6. Summary of Section II

For most of the semi-analytical models used to interpret hysteretic nonlinear wave propagation in damaged materials, we have identified the underlying PM-space formulation. In the simplest cases the PM-space density is constant, either over the entire PM-space or over distinct parts of the PM-space. In the Nazarov quadratic model with $\beta_1 + \beta_2 \neq 2\alpha$, an additional non-hysteretic memory dependent contribution is required to be taken into account.

Despite the ease of use, it is important to note that the semi-analytical formulations are only valid for simplex waves with only one minimum ($-\Delta\varepsilon$) and one maximum ($\Delta\varepsilon$) per excitation cycle. The more general PM-space formalism can extend these semi-analytical formulations to any arbitrary protocol.

The above analysis also shows that for a general PM-density (e.g. a superposition of the Granato-Lücke "split" density, the quadratic nonlinear hysteretic "constant" density, and the Davidenkov "powerlaw" increase of density from the diagonal),

- the modulus change will not be linear in the strain, but its dependence may be more complex, involving $\Delta\varepsilon$, $(\Delta\varepsilon)^2$, etc.,
- the change in the attenuation will not be linear in the strain, but its dependence may be more complex, involving $\Delta\varepsilon$, $(\Delta\varepsilon)^2$, etc.
- the theoretical Read parameter, providing information regarding the importance of nonlinear attenuation versus nonlinear modulus reduction, can take on a large range of values depending on the model parameters. In more complex cases (extended models) it is even possible for the Read parameter to become amplitude dependent.

III. Models for localized damage:

1. Clapping nonlinearity at the interface

For the description of interface or contact nonlinearity, the nonlinear stress-strain relations are implemented at the interface between two neighboring parts of the sample. Several research teams have realized this by introducing virtual spring elements and dampers at both sides of the interface [37-42]. In this contribution we illustrate the effect of local nonlinearity at delaminations and surface cracks following the method introduced by Sarens et al and Delrue et al. (Figure 7 and 8) [41,42]. The spring elements are only active when the interfaces are within a certain characteristic gap distance bZ_0, with Z_0 the common rest distance between molecules, and b>1. When the gap distance is smaller than Z_0, a repulsive force is exerted on both interfaces. When the gap distance is between Z_0 and bZ_0, the forces are attractive. No force and thus stress-free contacts are assumed when the gap distance is larger than bZ_0. The damping forces are defined in such a way that they always counteract the gap decrease or increase.

To verify the effect of the localized clapping nonlinearity on the macroscopic wave propagation, we implemented the spring and damper forces as boundary conditions in the commercial FEM software Comsol. As an example we consider a beam with a semi-circular surface-breaking crack (Figure 9). The spring and damper elements are only introduced at the interface. Figure 9 shows the in-plane x displacement for two points at either side of the interface, and illustrates the clapping effect (at certain periods during one cycle, the interfaces either loose contact or move along). Due to the clapping, nonlinearity is generated at the interface which is evidenced by the frequency analysis of the time signals through the creation of higher harmonics.

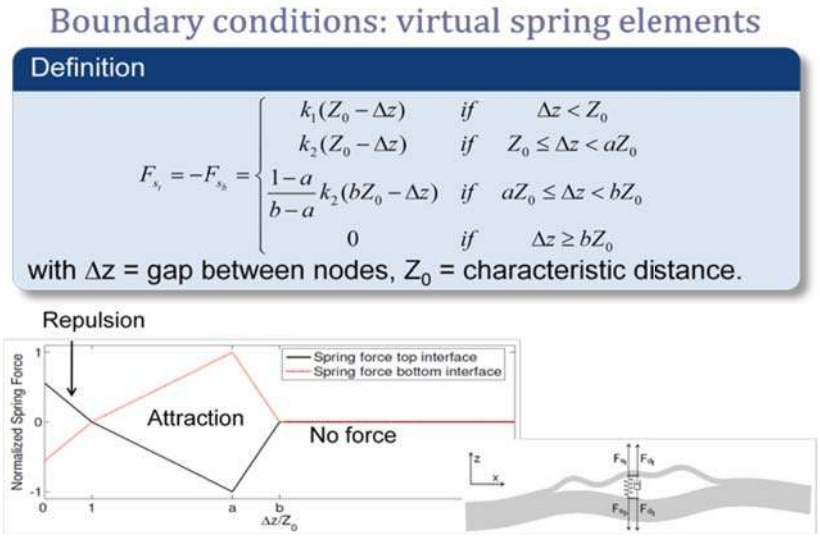

Figure 7: Definition of the nonlinear virtual spring elements at the interface of a delamination/crack.

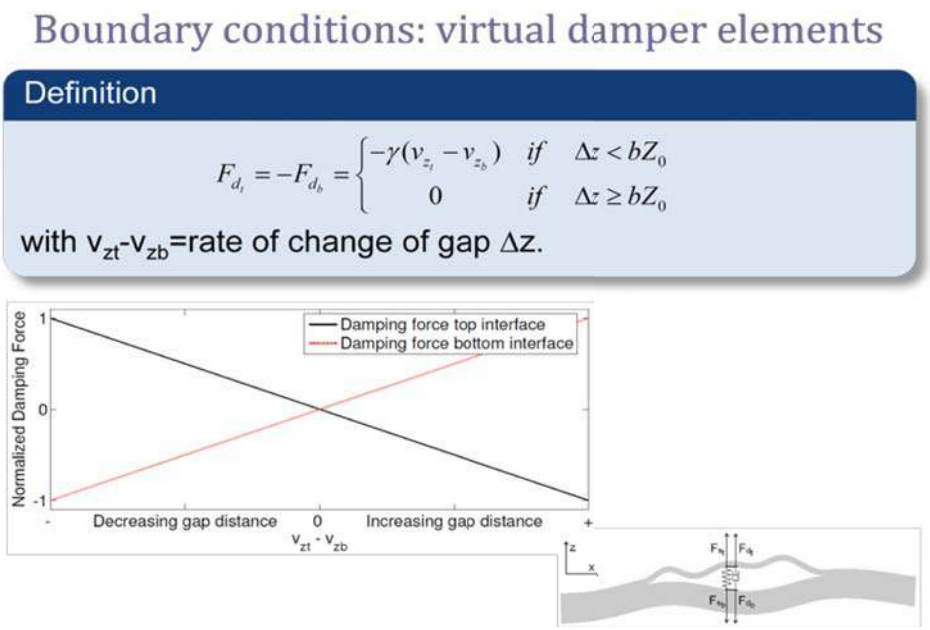

Figure 8: Definition of the virtual damper elements at the interface of a delamination/crack.

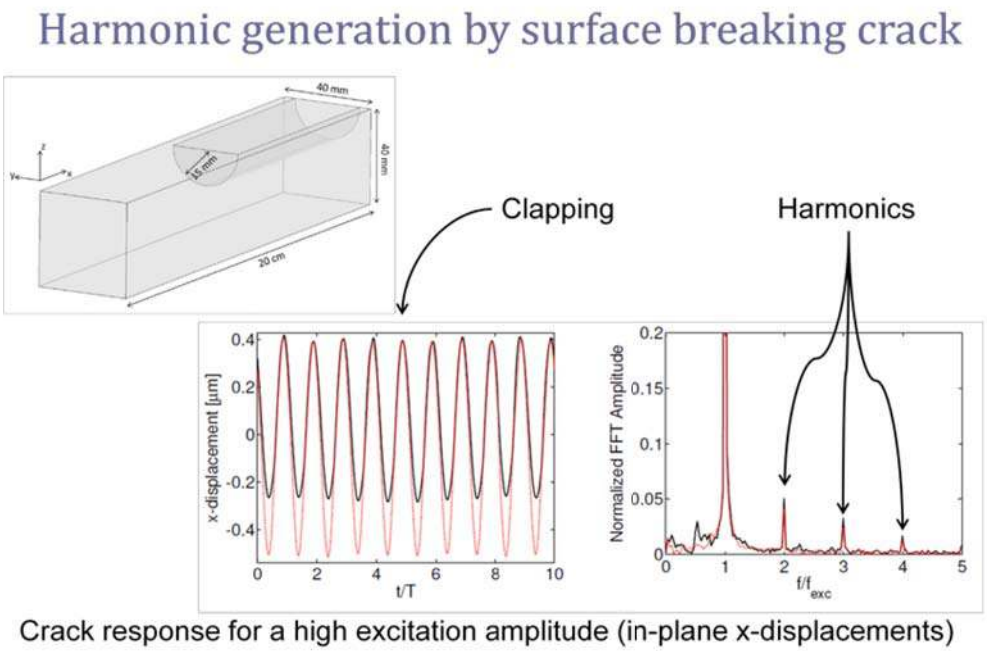

Figure 9: Surface breaking crack simulation, illustrating the clapping effect and the generation of harmonics.

The amplitudes of the generated harmonics can be scanned over the top surface of the beam. Figure 10 illustrates the distribution of the harmonic energy, which appears to be highly localized around the crack location.

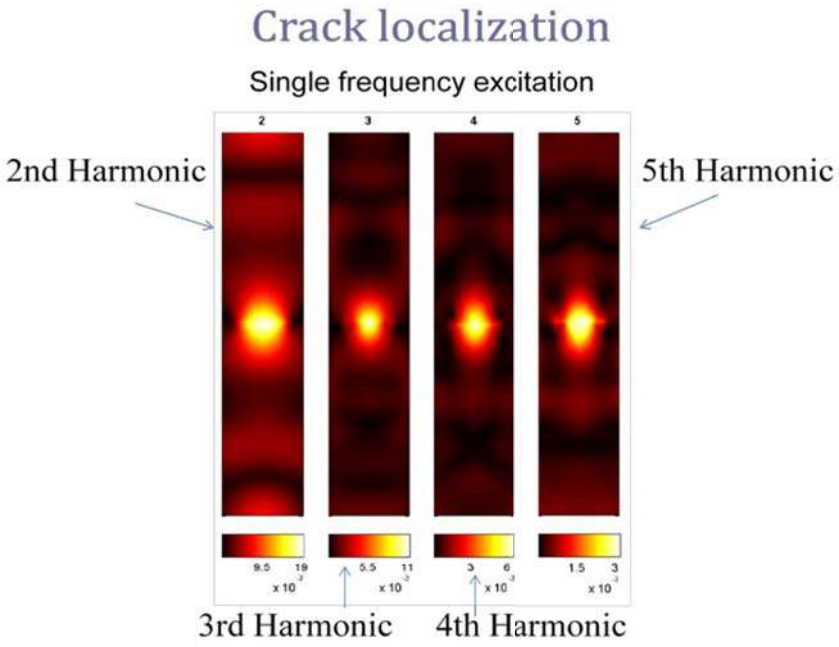

Figure 10: Interface scans of selected harmonics along the top surface of the beam. Excitation frequency is 22 kHz.

2. Nonlinear Air Coupled Emission

Solodov et al. exploited the high localisation of nonlinear energy for surface breaking cracks and delaminations close to the surface by investigating the nonlinear air-coupled emission of such defects using an acousto-optic measurement or an air-coupled transducer [33,34,35,36]. As illustrated in Figure 11, the interaction of leaky lamb waves with the defects produces a distinctive diffraction pattern for the various harmonics starting at the crack location, whereas this is not visible in the pattern of the fundamental frequency.

Using the Comsol code with implementation of the above discussed nonlinear interaction forces at the crack interfaces, we performed a qualitative simulation of the experiments reported by Solodov et al. [35]. The procedure for the coupled solid-air model is as follows: 1) 3D time domain simulation of the nonlinear wave propagation within the solid structure providing the 3D displacement at all points, 2) selection of the out of plane boundary signals at a line along the top interface and filtering around the fundamental or around one of the harmonics, and 3) calculation of the radiation pattern into the air using a frequency domain solver for the pressure in 2D.

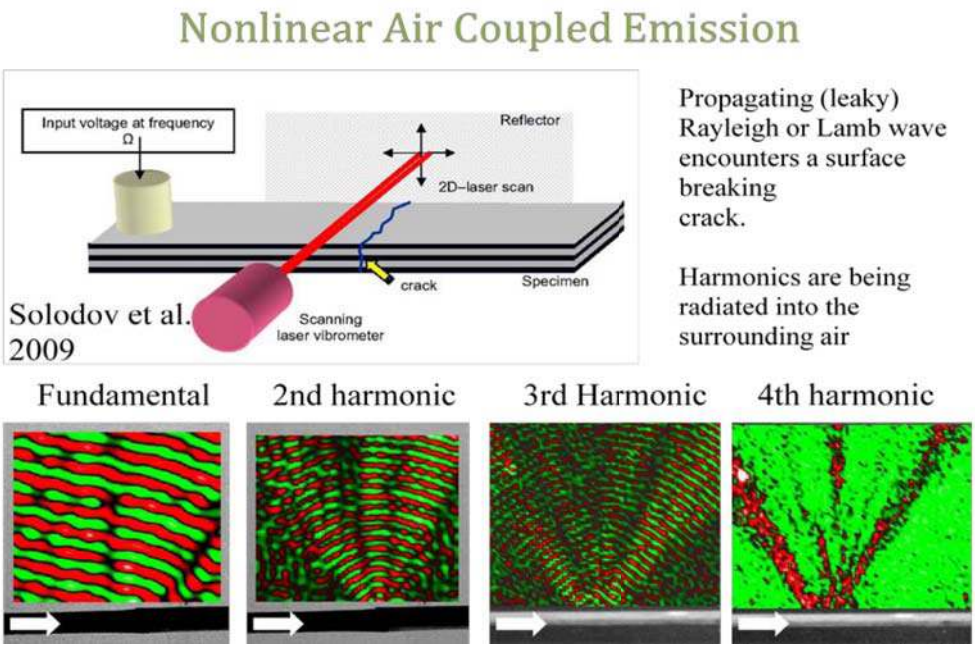

Figure 11: Principle and results of nonlinear air-coupled emission experiments at a surface breaking crack (from Solodov et al. [35]).

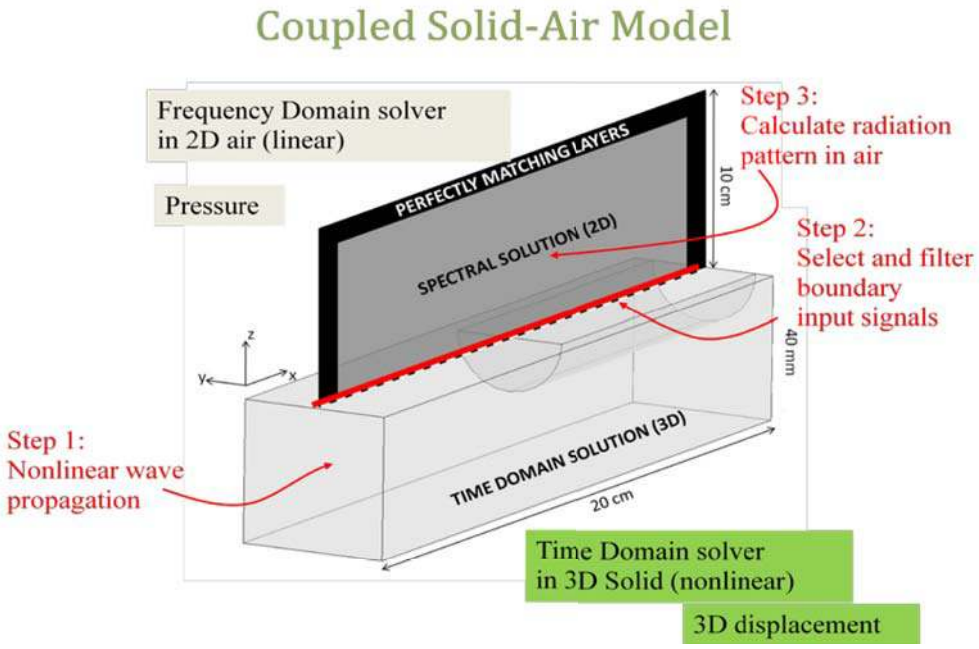

Figure 12: Simulation procedure for nonlinear air-coupled emission at a surface breaking crack.

The results of the coupled model are displayed in Figures 13-16. In all figures, as indicated in Figure 13, the analysis zone concerns a 2D zone in air perpendicularly above the plate, either across the surface breaking crack, or at the side of the crack location. When selecting the fundamental frequency component (Figure 14), the results show no evidence of the crack location in the emission pattern. Both positions give qualitatively the same results. For the second harmonic (Figure 15), there is clear evidence of a diffraction pattern at the crack location. For a position aside the crack the particular radiation pattern disappears. Similar results hold for the third harmonic (Figure 16). These results are qualitatively in agreement with the experimental observations reported by Solodov et al. [35].

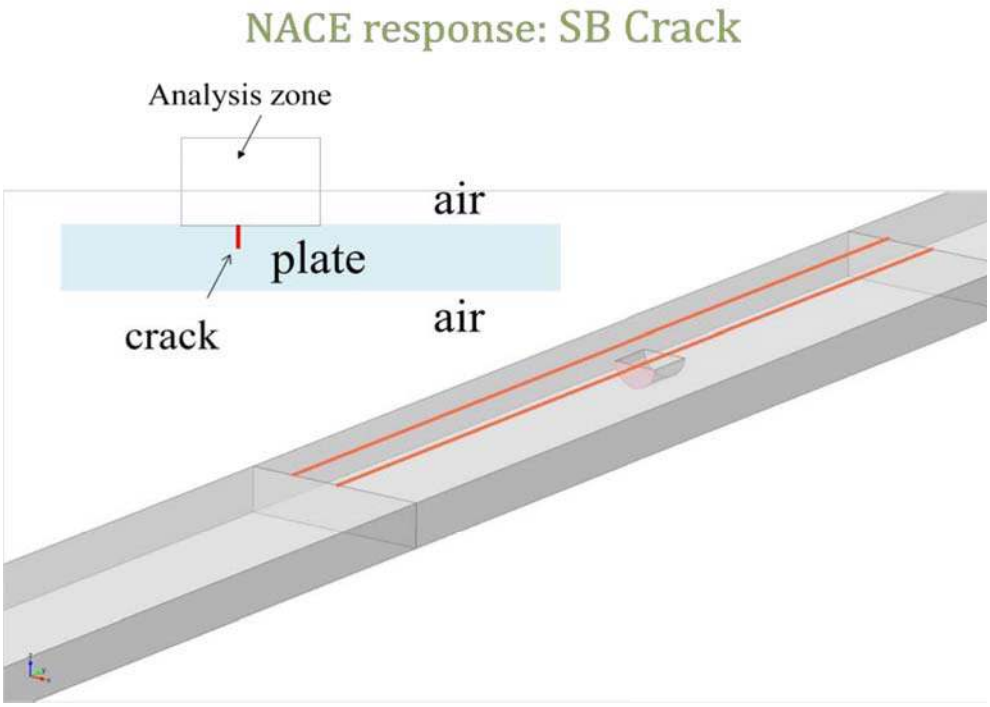

Figure 13: Analysis zone for the air-coupled emission simulation, and the two considered positions on the beam top surface

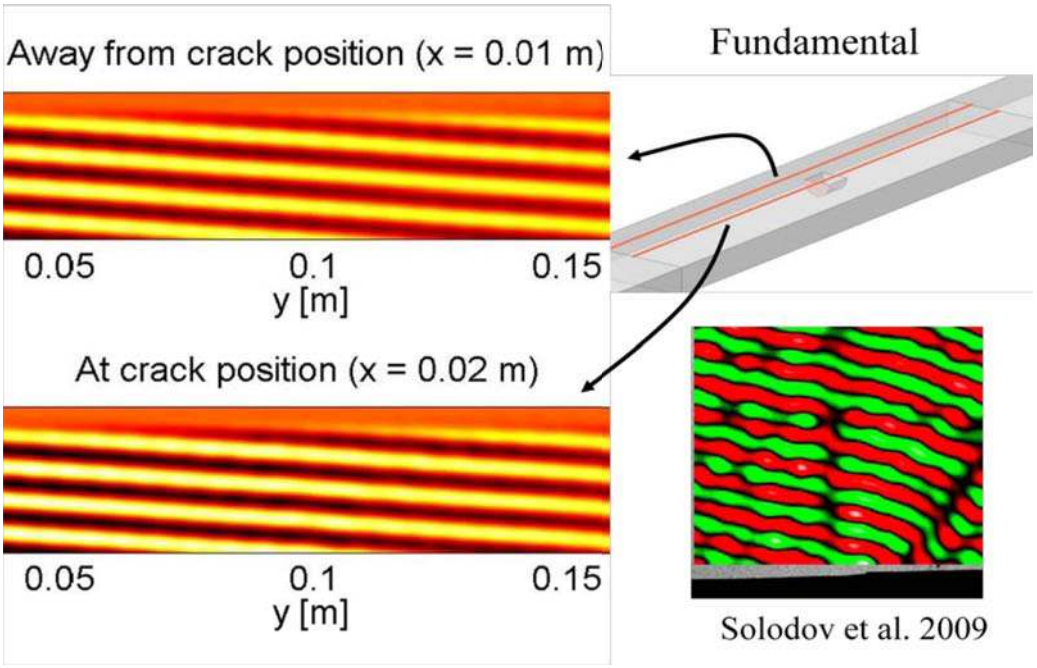

Figure 14: Radiation pattern for the fundamental frequency within the analysis zone above and aside the crack position. Qualitative comparison with the experiment of Solodov et al. [35].

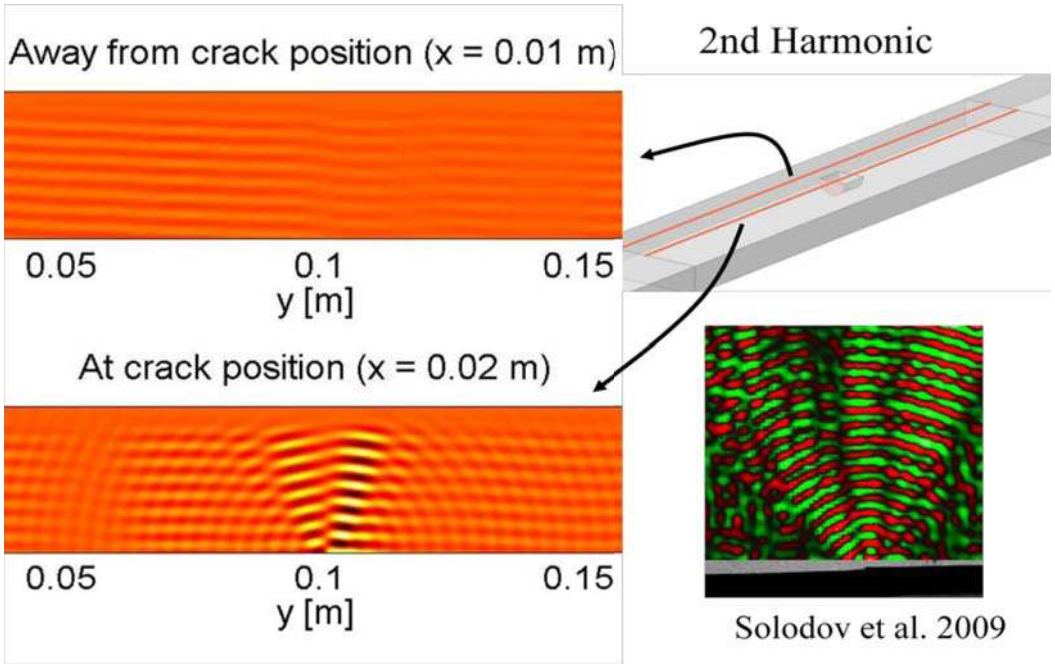

Figure 15: Radiation pattern for the second harmonic within the analysis zone above and aside the crack position. Qualitative comparison with the experiment of Solodov et al. [35].

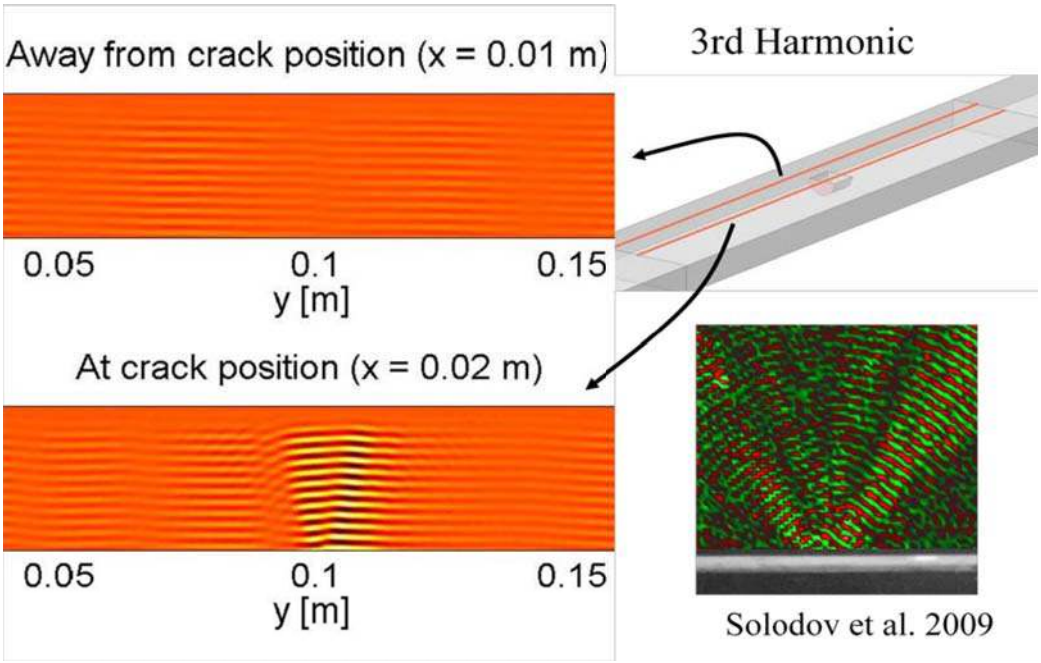

Figure 16: Radiation pattern for the third harmonic within the analysis zone above and aside the crack position. Qualitative comparison with the experiment of Solodov et al. [35].

3. Extension to hysteretic clapping

The above model assumes a perfect reversible force displacement relation. Due to friction and stick-clip effects, one can imagine that hysteresis should be accounted for. As an extension of the model we are currently adapting the simulation tool to accommodate hysteresis effects in the spring elements. Figure 17 provides an illustration of how this might be possible. Results of this model are forthcoming.

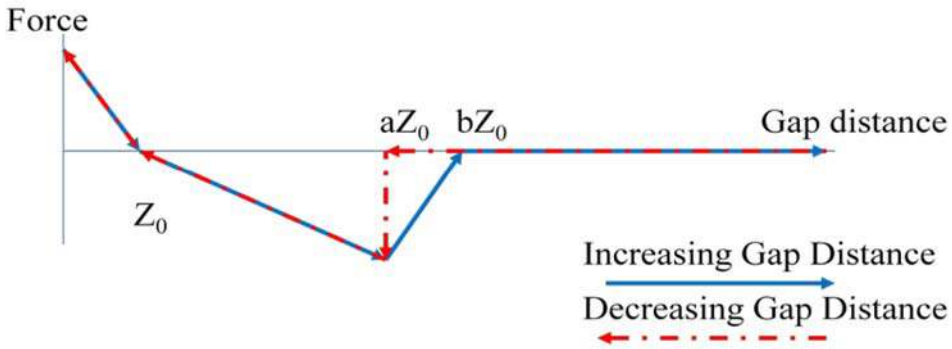

Figure 17: Potential extension of the local interface model to accommodate effects of hysteresis.

4. Summary of Section III

In contrast to distributed models, local interface models introduce nonlinearity at the level of the interface. Simple models can account for the experimentally observed clapping behavior of surface breaking cracks and delaminations. By coupling the time domain nonlinear model to a frequency domain linear radiation model, we have been able to make a qualitative comparison between the nonlinear air-coupled emission seen in experiments and predicted by our simulations. The models have the potential to be extended to accommodate effects of hysteresis due to friction and stick-slip.

IV. References

1 Landau, L., and Lifshitz, E. (1986). Theory of Elasticity. Pergammon (Oxford, UK).
2 Davidenkov, N. (1938). "Energy dissipation in vibrations," Journal of Technical Physics 8.
3 Lebedev, A. B. (1999). "Amplitude-dependent elastic-modulus defect in the main dislocation hysteresis models," Physics of the Solid State 41, 1105-1111.
4 Asano, S. (1970). "Theory of nonlinear damping due to dislocation hysteresis," Journal of the Physical Society of Japan 29, 952-&.
5 Granato, A., and Lucke, K. (1956). "Theory of mechanical damping due to dislocations," Journal of Applied Physics 27, 583-593.
6 Nazarov, V. E., Kolpakov, A. B., and Radostin, A. V. (2009). "Amplitude dependent internal friction and generation of harmonics in granite resonator," Acoustical Physics 55, 100-107.
7 Nazarov, V. E. (1991a). "Nonlinear acoustical effects in annealed copper," Soviet Physics Acoustics-Ussr 37, 75-78.
8 Nazarov, V. E. (1999). "Amplitude-dependent internal friction of lead," Fizika Metallov I Metallovedenie 88, 82-90.
9 Nazarov, V. E. (2001b). "Experimental investigation of amplitude-dependent internal friction of polycrystalline zinc," Physics of Metals and Metallography 92, 592-601.
10 Nazarov, V. E., and Kolpakov, A. B. (2000). "Experimental investigations of nonlinear acoustic phenomena in polycrystalline zinc," Journal of the Acoustical Society of America 107, 1915-1921.
11 Nazarov, V. E., Ostrovsky, L. A., Soustova, I. A., and Sutin, A. M. (1988). "Nonlinear Acoustics of Micro-Inhomogeneous Media," Physics of the Earth and Planetary Interiors 50, 65-73.
12 Nazarov, V. E., Radostin, A. V., Ostrovsky, L. A., and Soustova, I. A. (2003). "Wave processes in media with hysteretic nonlinearity. Part I," Acoustical Physics 49, 344-353.
13 Ortin, J "Preisach modeling of hysteresis for a pseudoelastic cu-zn-al single-crystal " J. Applied Physics 71, 3, 1454-1461
14 McCall, K., and Guyer, R. (1996). "A new theoretical paradigm to describe hysteresis, discrete memory and nonlinear elastic wave propagation in rock," Nonlinear processes in geophysics 3, 89-101.
15 McCall, K. R., and Guyer, R. A. (1994). "Equation of State and Wave-Propagation in Hysteretic Nonlinear Elastic-Materials," Journal of Geophysical Research-Solid Earth 99, 23887-23897.
16 Guyer, R. A., McCall, K. R., and Boitnott, G. N. (1995). "Hysteresis, Discrete Memory, and Nonlinear-Wave Propagation in Rock - a New Paradigm," Physical Review Letters 74, 3491-3494.
17 Capogrosso-Sansone, B., and Guyer, R. (2002). "Dynamic model of hysteretic elastic systems," Physical Review B 66, 224101.
18 Van Den Abeele, K. (2007). "Multi-mode nonlinear resonance ultrasound spectroscopy for defect imaging: An analytical approach for the one-dimensional case," Journal of the Acoustical Society of America 122, 73-90.
19 Van Den Abeele, K. E. A., Carmeliet, J., Ten Cate, J. A., and Johnson, P. A. (2000b). "Nonlinear elastic wave spectroscopy (NEWS) techniques to discern material damage, Part II: Single-mode nonlinear resonance acoustic spectroscopy," Research in Nondestructive Evaluation 12, 31-42.
20 Van Den Abeele, K. E. A., Johnson, P. A., and Sutin, A. (2000c). "Nonlinear elastic wave spectroscopy (NEWS) techniques to discern material damage, part I: Nonlinear wave modulation spectroscopy (NWMS)," Research in Nondestructive Evaluation 12, 17-30.
21 Johnson, P., and Sutin, A. (2005). "Slow dynamics and anomalous nonlinear fast dynamics in diverse solids," Journal of the Acoustical Society of America 117, 124-130.
22 Read, T. A. (1940). "The internal friction of single metal crystals," Physical Review 58, 371-380.
23 Read, T. A. (1941). "Internal friction of single crystals of copper and zinc," Met Technol 8, 1-12.
24 Haupert, S., G. G. Renaud, J. Riviere, M. Talmant, P. Johnson and P. Laugier (2011) High-accuracy acoustic detection of non-classical component of material nonlinearity., J. Acoust. Soc. Am. 130, 2654-2661 DOI:10.1121/1.3641405

25 Scalerandi, M., Gliozzi, A., Bruno, C., and Antonaci, P. (2010). "Nonequilibrium and hysteresis in solids: Disentangling conditioning from nonlinear elasticity," Physical Review B 81, 104114.
26 Nobili, M., and Scalerandi, M. (2004). "Temperature effects on the elastic properties of hysteretic elastic media: Modeling and simulations," Physical Review B 69, 104105.
27 Gusev, V., and Tournat, V. (2005). "Amplitude- and frequency-dependent nonlinearities in the presence of thermally-induced transitions in the Preisach model of acoustic hysteresis," Physical Review B 72.
28 Solodov, I., Pfleiderer, K., and Busse, G. (2006). "Nonlinear acoustic NDE: inherent potential of complete nonclassical spectra," Universality of Nonclassical Nonlinearity, 467-486.
29 Solodov, I. Y. (1998). "Ultrasonics of non-linear contacts: propagation, reflection and NDE-applications," Ultrasonics 36, 383-390.
30 Solodov, I. Y., Krohn, N., and Busse, G. (2002). "CAN: an example of nonclassical acoustic nonlinearity in solids," Ultrasonics 40, 621-625.
31 Korshak, B., Solodov, I. & Ballad, E. 2002. DC effects, sub-harmonics, stochasiticy and “memory” for contact acoustic non-linearity. Ultrasonics 40: 707-713.
32 Krohn, N., Stoessel, R. & Busse, G. 2002. Acoustic non-linearity for defect selective imaging. Ultrasonics 40: 633-637.
33 Solodov, I., Döring, D., and Busse, G. "Air-coupled vibrometry for measurements in classical and nonclassical nonlinear acoustics". In Proceedings of the XIV International Conference on Nonlinear Elasticity in Materials (Lisbon, June 2009).
34 Solodov, I., Döring, D., and Busse, G. "Classical and non-classical nonlinear effects discerned by airborne ultrasound. " Proceedings of the 20th international congress on Acoustics, ICA 2010 (Sydney, August 2010).
35 Solodov, I., and Busse, G. Nonlinear air-coupled emission: The signature to reveal and image microdamage in solid materials. Appl. Phys. Lett. 91 (2007), 251910
36 Igor Solodov, Juxing Bai, Sumbat Bekgulyan, and Gerd Busse "A local defect resonance to enhance acoustic wave-defect interaction in ultrasonic nondestructive evaluation", Appl. Phys. Lett. 99, 211911 (2011); doi: 10.1063/1.3663872
37 K. Yamanaka, Y. Shintaku, Y. Ohara, “Two Dimensional Model for Subharmonic Generation at Closed Cracks with Damped Double Nodes” AIP Conference Proceedings (ISNA 2012; Nonlinear Acoustics State-of-the-Art and Perspectives), 1474 (2012) 179-182.
38 Y. Ohara, Y. Shintaku, S. Horinouchi, M. Ikeuchi, K. Yamanaka “Analysis on Nonlinear Ultrasonic Imaging of Closed Cracks by Damped Double Node Model” Proceedings of Symposium on Ultrasonic Electronics, 32 (2011) 31-32.
39 K. Yamanaka, Y. Ohara, M. Oguma, Y. Shintaku “Two-Dimensional Analyses of Subharmonic Generation at Closed Cracks in Nonlinear Ultrasonics” Applied Physics Express, 4 (2011) 076601-1-3.
40 K. Yamanaka, R. Sasaki, T. Ogata, Y. Ohara, T. Mihara “Time Domain Analysis of Subharmonic Ultrasound for Practical Crack Sizing” Review of Progress in Quantitative Nondestructive Evaluation, 25 (2006) 283-290.
41 Delrue, S., Van Den Abeele, K. (2012). "Three-dimensional finite element simulation of closed delaminations in composite materials", Ultrasonics, 52(2), 315-324.
42 Sarens, B., Verstraeten, B., Glorieux, C., Kalogiannakis, G., and Van Hemelrijck, D. 2010. Investigation of contact acoustic nonlinearity in delaminations by shearographic imaging, laser doppler vibrometric scanning and finite difference modeling. IEEE T. Ultrason. Ferr. 57: 1383–1395.
43 Aleshin, V., Van Den Abeele, K. (2012). Hertz-Mindlin problem for arbitrary oblique 2D loading: General solution by memory diagrams. Journal of the Mechanics and Physics of Solids, 60(1), 14-36.
44 Aleshin, V., Van Den Abeele, K. (2009). Preisach analysis of the Hertz-Mindlin system. Journal of the mechanics and physics of solids, 57 (4), 657-672.

45 Aleshin, V., Desadeleer, W., Wevers, M., Van Den Abeele, K. (2008). Characterization of hysteretic stress-strain behavior using the integrated Preisach density. International journal of non-linear mechanics, 43 (3), 151-163.
46 Aleshin, V. and Van Den Abeele, K. (2007). "Friction in unconforming grain contacts as a mechanism for tensorial stress-strain hysteresis," Journal of the Mechanics and Physics of Solids 55, 765-787.
47 Aleshin, V. and Van Den Abeele, K. (2007). "Microcontact-based theory for acoustics in microdamaged materials," Journal of the Mechanics and Physics of Solids 55, 366-390.
48 Aleshin, V., Van Den Abeele, K. (2005). Micro-potential model for stress-strain hysteresis of micro-cracked materials. Journal of the mechanics and physics of solids, 53(4), 795-824.
49 Pecorari, C. (2004). "Adhesion and nonlinear scattering by rough surfaces in contact: Beyond the phenomenology of the Preisach–Mayergoyz framework," The Journal of the Acoustical Society of America 116, 1938.
50 Scalerandi, M., Gliozzi, A., Bruno, C., Masera, D. & Bocca, P. 2008. A scaling subtraction method to enhance detection of a nonlinear elastic response. Appl. Phys. Lett. 92.